TMR4205 Buckling and Ultimate Strength of Marine Structures

Chapter 3:
Buckling of Stiffened Plates

by
Professor Jørgen Amdahl

MTS-2009.05.18

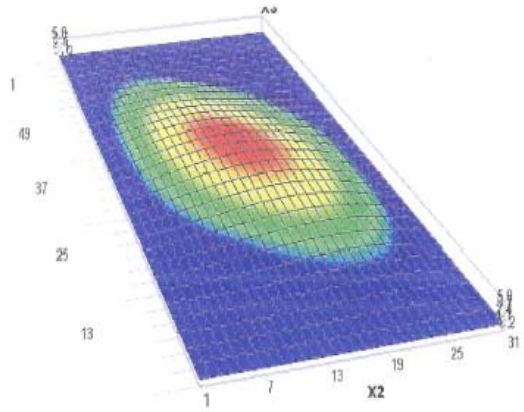

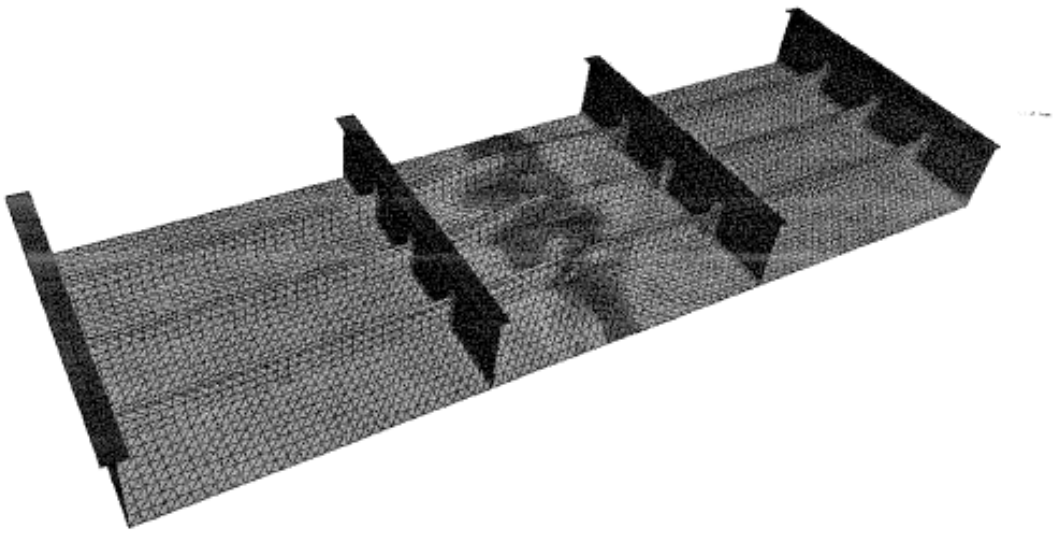

CONTENTS

3. BUCKLING OF STIFFENED PLATES

3. BUCKLING OF STIFFENED PLATES

3.1 Introduction

Stiffened plates are frequently used as structural components in marine structures. Typical examples are the hull girder and superstructure of a ship, the pontoons of a semi-submersible and the deck of offshore platforms.

The main type of framing system found in hull girders consists of relatively closely spaced longitudinal stiffeners with more widely spaced heavier girders in the transverse direction. This is illustrated for a bottom/side structure in Figure 3.1.

The main purpose of the plates is to transfer the hydrostatic loads (the difference between external and internal pressure) to the stiffeners, which again, through beam action, transfer the loads to the transverse girders. These are parts of the transverse frames of the hull girder. From the vertical girders the loads are introduced as membrane stresses in the side. The side will also be subjected to hydrostatic loads.

In general the bottom plate will, in addition to the hydrostatic pressure, be subjected to biaxial in-plane loads caused by longitudinal bending of the hull girder and from the hydrostatic pressure on the sides as illustrated in Figure 3.1.

It is very difficult to perform rigorous analysis of such panels subjected to simultaneous action of lateral pressure as well as in-plane loads. For design purposes, the problem is often split such that the critical load is first determined for each of the loads acting alone. The critical load for the combined loading is found by means of some interaction formula.

Parameters of major importance for the behaviour of stiffened plates are:-

- length/width ratio of the panel
- stiffener geometry and spacing
- aspect ratio for plate between stiffener
- plate slenderness
- residual stresses
- initial distortions
- boundary conditions
- type of loading

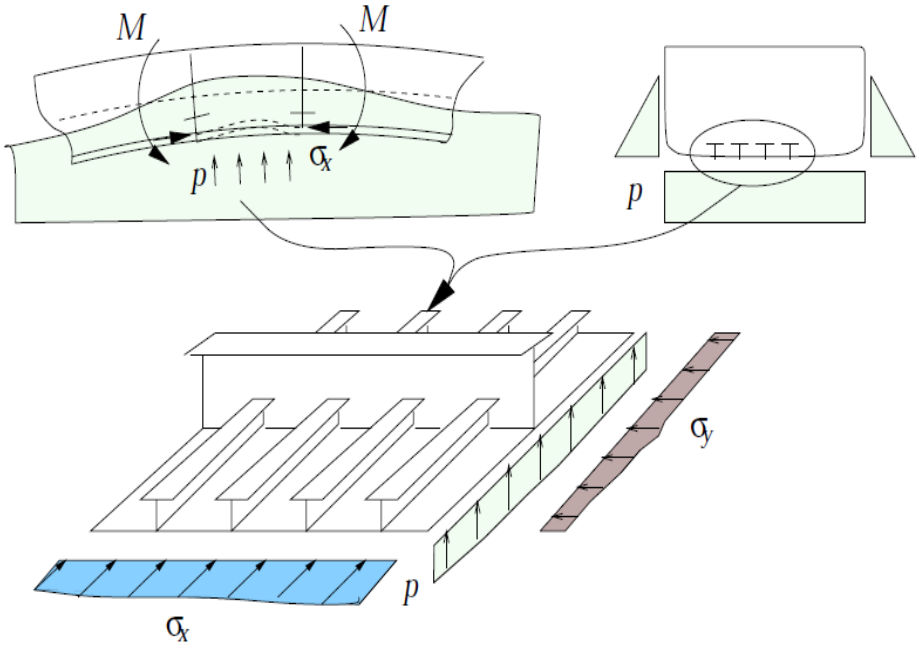

Figure 3.1 Stiffened Panels in a Bottom Structure, (Interaction Between Global and Local Loads).

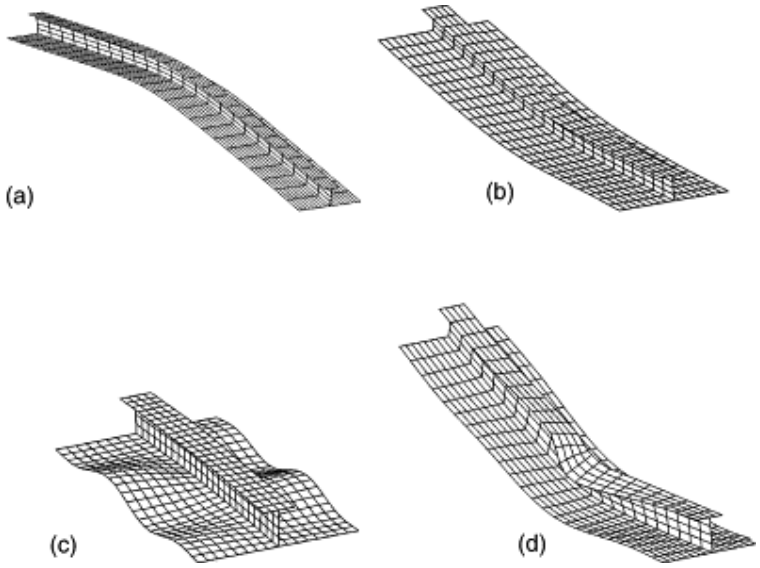

The possible failure modes of a stiffened panel under longitudinal compression may be classified as follows:

- ***Plate buckling and ultimate collapse***, which means that the maximum plate load is exceeded and is followed by unloading of the plate, leading to collapse of the stiffened panel before significant yield occurs in the stiffeners.

- ***Interframe flexural buckling*** of the longitudinal stiffeners with associated plating. This type of failure involves yielding of the stiffeners, which is accelerated by loss of stiffness due to buckling or yielding of the plate.

- ***Restrained torsional buckling of stiffeners*** (see Section 4.8), which is due to elastic or elasto-plastic loss of stiffness depending on the slenderness of the stiffeners, the rotational restraint provided by the plating, and the initial out-of-shape.

- ***Overall grillage buckling***, which involves bending of transverse girders as well as longitudinal stiffeners.

Most structures are designed to prevent overall grillage buckling. Therefore, this failure mode is unlikely except for lightly stiffened panels found in superstructure decks.

For short panels, local plate buckling may be the critical mode. It will be shown, however, that plates, depending on the boundary conditions, possess significant reserve strength as indicated in Figure 3.2c. This reserve strength may be taken into account in the design of stiffened panels by allowing the plate to deform into the post-buckling region, but it has to be assured that local buckling does not occur frequently. Repetitive buckling and straightening under cyclic loading may lead to (extreme) low cycle fatigue failure.

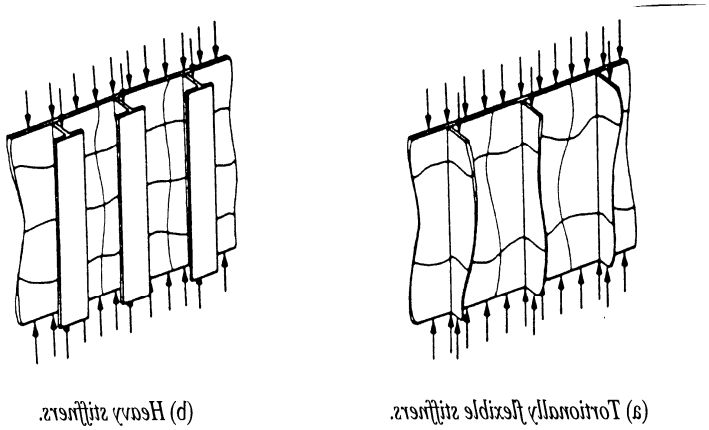

(c) Load-deflection behaviour of plate element.

Figure 3.2 Buckling of Short Panel.

The post-buckling behaviour of the plate depends heavily on the boundary conditions. Important interactions can occur between stiffeners and the plate. Torsionally flexible stiffeners will twist in accordance with the plate buckling mode as shown in Figure 3.2a. In the case of heavy

stiffeners (Figure 3.2b) considerable redistribution of loads is possible in the post-buckling phase, which gives an increasing load-carrying capacity as indicated in Figure 3.2c.

For a long panel inter-frame flexural buckling of the stiffener with associated plate flange becomes a potential failure mode. Panels with heavy stiffeners will follow a column mode of collapse (Figure 3.3a). The associated load-deflection characteristic is shown in Figure 3.3b. However, if buckling occurs with the stiffeners in compression, flexible stiffeners will be susceptible to restrained torsional buckling. The interaction between the two failure modes may lead to a dramatic unloading in the post-collapse region (Figure 3.3c).

One might suggest that the optimum way of designing a panel is to require equal capacity against local buckling and inter-frame flexural buckling, (see Figure 3.4a). Owing to interaction effects between the two modes, the elastic buckling load is reduced as compared to the Euler load. The *optimum* panel is also very imperfection sensitive (Figure 3.4b).

A vast amount of research has been carried out on the behaviour of stiffened plates. Analytic work has mainly dealt with ideal structures. However, the development of non-linear computer programs has rendered possible in-depth studies of the effect of different imperfections. A review is given in /7.1/. However, for design purposes simplified procedures calibrated against experiments or numerical studies, should be available. In the remainder of this section some of the most important methods are presented.

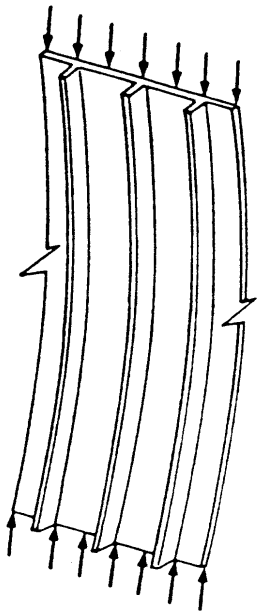

(a) *Buckling mode.*

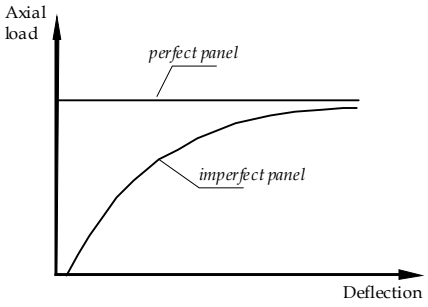

(b) *Heavy stiffeners.*

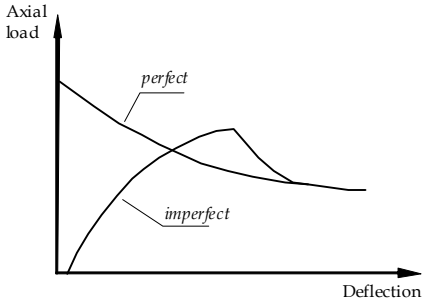

(c) *Torsional buckling of stiffeners.*

Figure 3.3 Buckling of Long Panel.

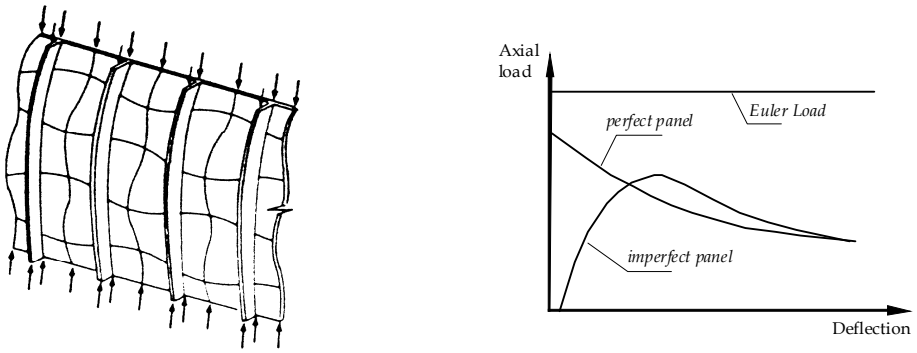

(a) ***Buckling mode.*** (b) *Load-deflection behaviour.*

Figure 3.4 Buckling of *Optimum* Panel.

3.2 Local Plate Buckling

The classical approach to elastic plate buckling problems is either by solving the differential equation of equilibrium or applying energy methods.

3.2.1 Elastic Buckling of Initially Perfect Plates

Solution of the differential equation

The procedure for calculating the elastic buckling load is illustrated for an initially plane plate subjected to in-plane uniform compression. The equilibrium equation for a plate is given by /7.1/

$$\nabla^4 w = \frac{1}{D}\left(q + N_x \frac{\partial^2 w}{\partial x^2} + 2N_{xy} \frac{\partial^2 w}{\partial x \partial y} + N_y \frac{\partial^2 w}{\partial y^2} \right) \tag{3.1}$$

where the plate stiffness is given by,

$$D = \frac{Et^3}{12\left(1-\nu^2\right)} \tag{3.2}$$

and,

$$\nabla^4 = \left(\nabla^2\right)^2 = \left(\frac{\partial^2}{\partial x^2} + \frac{\partial^2}{\partial y^2} \right)^2 \tag{3.3}$$

The quantities,

$$\left.\begin{aligned} N_x &= \sigma_x t \\ N_y &= \sigma_y t \\ N_{xy} &= \sigma_{xy} t \end{aligned}\right\} \tag{3.4}$$

are the membrane stress resultants.

For uniaxial compression, simple supports and no external load, Equation (3.1) takes the form,

$$\nabla^4 w = \frac{N_x}{D} \frac{\partial^2 w}{\partial x^2} \tag{3.5}$$

The critical load results from the solution of the differential equation. The following displacement function satisfies Equation (3.5) and the boundary conditions,

$$w = C_{mn} \sin\frac{m\pi x}{a}\sin\frac{n\pi y}{b} \tag{3.6}$$

where *m* and *n* are number of half waves in the *x*- and *y*-directions, (see Figure 3.5). The solution is given by the expression,

$$\sigma_E = \frac{\pi^2 E}{12\left(1-\nu^2\right)}\left(\frac{t}{b}\right)^2 \cdot k \tag{3.7}$$

where *k* is a factor depending on the plate aspect ratio, (see Figure 3.6).

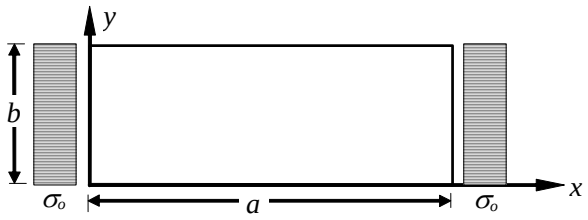

Figure 3.5 Simply Supported Plate Subjected to Uniform Compression.

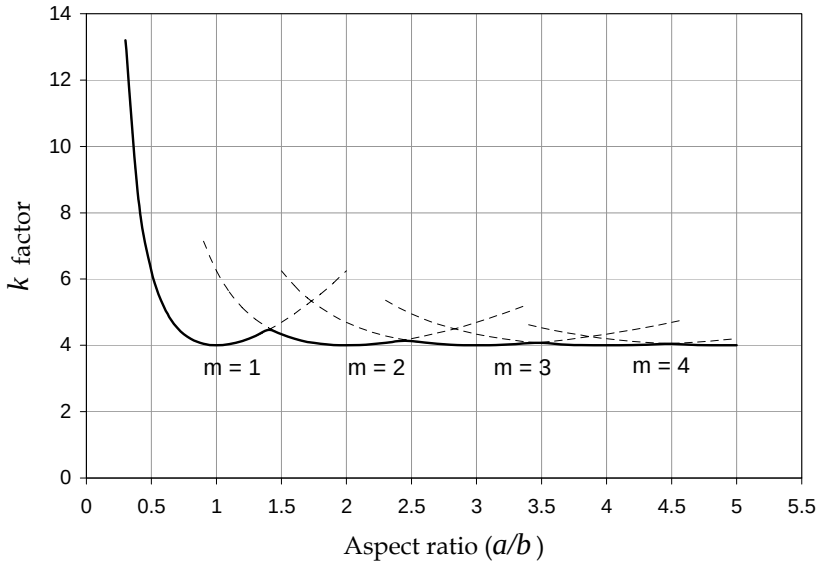

Figure 3.6 Buckling Coefficient versus Plate Aspect Ratio.

Solution by means of energy method

Alternatively, the energy method may be applied in the same way as demonstrated for column buckling in Section 5.2. The elastic strain energy caused by bending deformation of the plate at the critical load is given by,

$$U = \frac{D}{2}\int_0^a\int_0^b \left\{\left(\nabla^2 w\right)^2 - 2\left(1-\nu\right)\left(\frac{\partial^2 w}{\partial x^2}\frac{\partial^2 w}{\partial y^2} - \left(\frac{\partial^2 w}{\partial x \partial y}\right)^2\right)\right\} dx\,dy \tag{3.8}$$

It can be shown that the term in the last bracket in Equation (3.8) disappears if either of the two conditions are satisfied along the boundaries;

$$\text{i.)} \quad w = 0$$
$$\text{ii.)} \quad \frac{\partial w}{\partial n} = 0 \tag{3.9}$$

where $\square$ 2denotes the differentiation in the edge normal direction. The expression for the potential of external compressive load reads

$$H = -\frac{N_x}{2}\int_0^a\int_0^b\left(\frac{\partial w}{\partial x}\right)^2 dxdy \tag{3.10}$$

Then, the total potential energy becomes,

$$\Pi = U + H \tag{3.11}$$

The critical load is now found by applying the principle of minimum potential energy, i.e. by setting the *variation*;

$$\delta\Pi = \frac{\partial \Pi}{\partial C_i}\delta C_i = 0 \qquad i = 1, 2, ..., n \tag{3.12}$$

where C_i denotes the function amplitudes in the selected displacement field, w. In order to satisfy the above condition, all the derivatives have to vanish.

The accuracy of the energy methods, to predict the critical load, depends on the selected displacement functions. At least, the principal (essential) boundary conditions should be satisfied. Generally, the energy method yields a critical load greater or equal to the exact solution.

The ideal critical load can generally be written as,

$$\sigma_E = \frac{\pi^2 E}{12\left(1-\nu^2\right)}\left(\frac{t}{b}\right)^2 \cdot k \tag{3.13}$$

where k is a factor accounting for the aspect ratio, (a/b), the boundary conditions, and load the condition.

In Figure 3.6, the buckling coefficient k has been plotted against the aspect ratio for a simply supported plate subjected to uniform compression. It appears that the minimum buckling stress occurs when the length is a multiplum of the width. For intermediate values the number of waves is incompatible with the plate length, hence raising the buckling load somewhat. In practice, however, this additional strength is not taken into account.

In Figure 3.7 and Figure 3.8, the buckling coefficients are tabulated for various load and boundary conditions.

a.) Non-uniform compression $(0 \le \psi \le 1)$	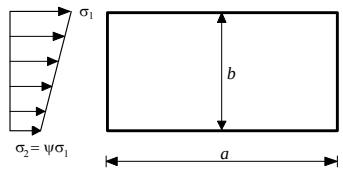	$k = \dfrac{8.4}{\psi + 1.1}$ $(\psi = 1 \quad : \quad k = 4)$
b.) Pure bending $(\psi = -1)$	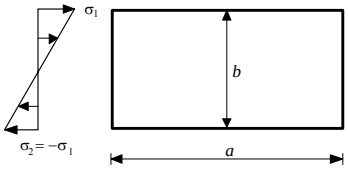	$k = 24$
c.) $(-1 < \psi < 0)$	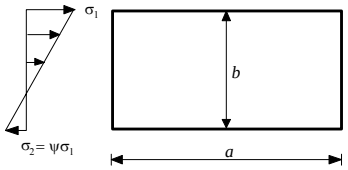	$k = 7.6 - 6.4\psi + 10\psi^2$
d.) Pure shear	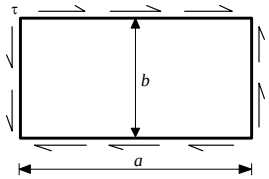	$k = 5.34 + 4\left(\dfrac{b}{a}\right)^2$
e.) Non-uniform compression $(0 \le \psi \le 1)$	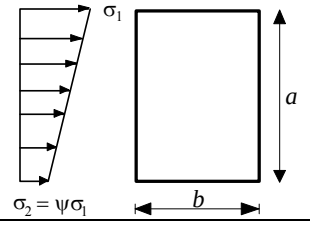	$k = \left[1 + \left(\dfrac{b}{a}\right)^2\right]^2 \dfrac{2.1}{\psi + 1.1}$ $\psi = 1 \quad : \quad k = \left[1 + \left(\dfrac{b}{a}\right)^2\right]^2$
f.) Pure bending 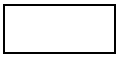	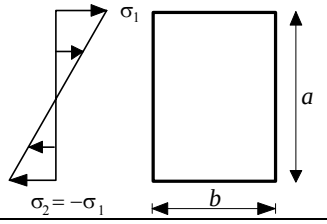	$\dfrac{a}{b} \le \dfrac{3}{2} := 24\left(\dfrac{b}{a}\right)^2$ $\dfrac{a}{b} > \dfrac{3}{2} := 2 + 16\left(\dfrac{b}{a}\right)^2 + 8\left(\dfrac{b}{a}\right)^4$
g.) 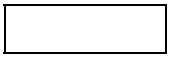	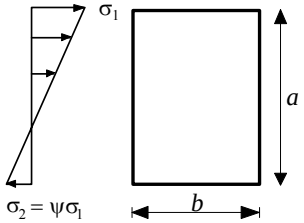	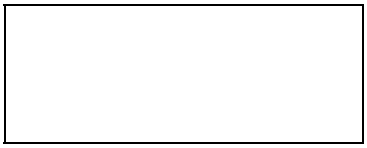

Figure 3.7 The Buckling Coefficients for Various Load Conditions.

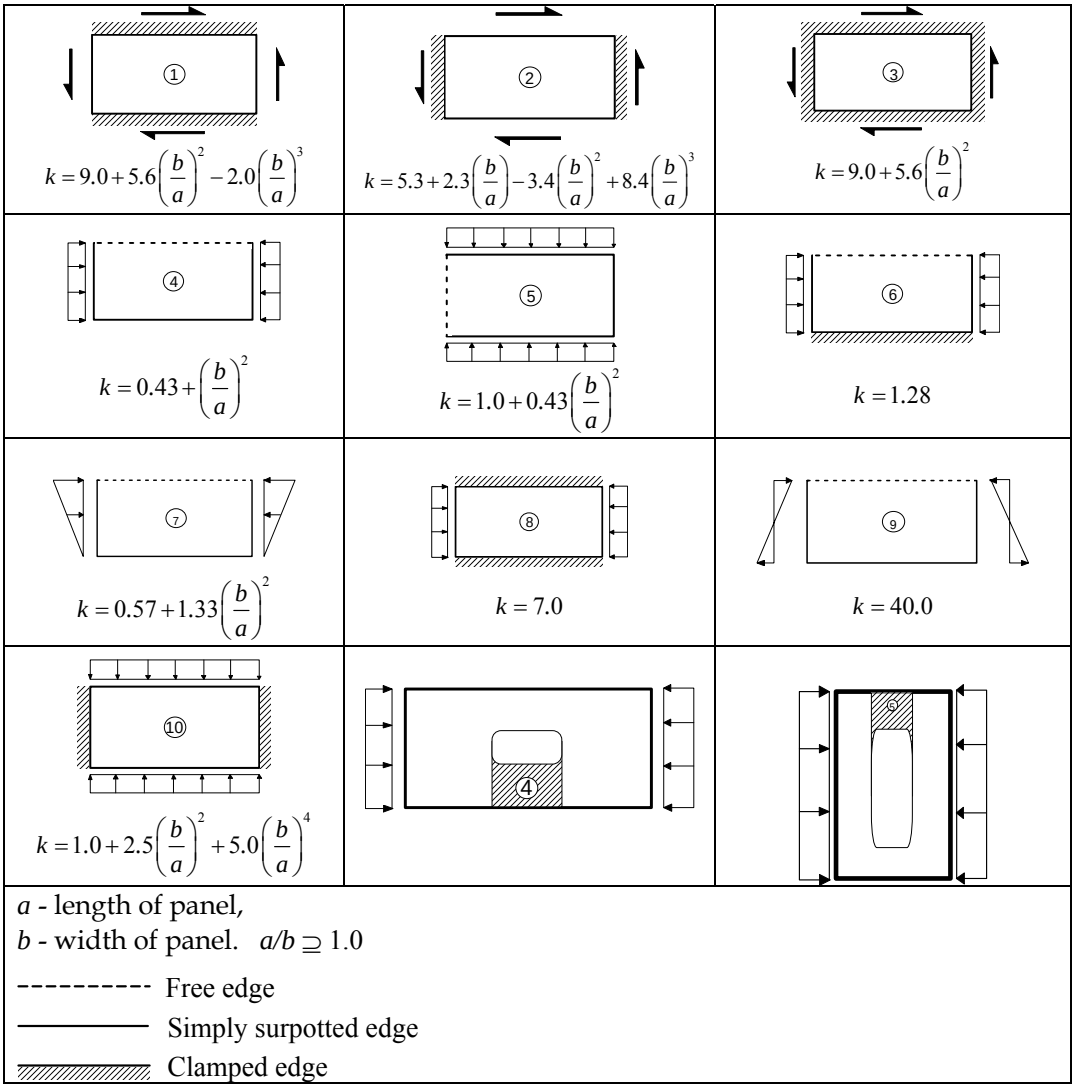

Figure 3.8 The Buckling Coefficient for Various Boundary Conditions.

3.2.2 Correction for Plasticity

For plates with a low *width to thickness* ratio, Equation (3.13) may predict a critical stress in excess of the yield stress, (see Figure 3.9), which is unphysical. Various methods exist to account for plasticity effects. A convenient technique for modifying the elastic critical stress due to plasticity is the ϕ-method, where the elastic-plastic buckling stress is given by,

$$\sigma_{cr} = \phi \cdot \sigma_Y \tag{3.14}$$

where ϕ is an empirical function related to the structural slenderness. Several parameters may be used, but the most general measure is the reduced slenderness ratio.

$$\overline{\lambda} = \sqrt{\frac{\sigma_Y}{\sigma_E}} \tag{3.15}$$

Various expressions for ϕ, exists. One method is to account for elasto-plastic effects by means of an elliptical interaction equation;

It is seen that,

$$\sigma_{cr} \to \sigma_Y \quad when \quad \sigma_E \to \infty$$
$$\sigma_{cr} \to \sigma_E \quad when \quad \sigma_E << \sigma_Y$$

Hence, the formula converges to the correct solution for both:- stocky members and slender members. Solving for σ_{cr}, we obtain,

$$\sigma_{cr} = \frac{\sigma_Y}{\sqrt{1+\bar{\lambda}^4}} \quad \Rightarrow \quad \phi = \frac{1}{\sqrt{1+\bar{\lambda}^4}} \tag{3.16}$$

Another well-known solution is the so called *Johnson-Ostenfeld* formula,

$$\phi = \begin{cases} 1 - \dfrac{\bar{\lambda}^2}{4} & , \quad \bar{\lambda}^2 \le 2 \\ \dfrac{1}{\bar{\lambda}^2} & , \quad \bar{\lambda}^2 \ge 2 \end{cases} \tag{3.17}$$

In the case of a combined loading, as shown in Figure 3.10, the above procedure may be applied provided that an equivalent stress and an equivalent elastic buckling stress are defined. The requirement is that the utilization for the equivalent stress should be equal to the utilization for the combined loading. This is conveniently expressed by the following interaction formula,

$$\left(\frac{\sigma_e}{\sigma_{Ee}}\right)^c = \left(\frac{\sigma_x}{\sigma_{Ex}}\right)^c + \left(\frac{\sigma_y}{\sigma_{Ey}}\right)^c + \left(\frac{\tau}{\tau_E}\right)^c \tag{3.18}$$

where σ_{Ex}, σ_{Ey}, and τ_E are the elastic buckling stresses when the corresponding stress component acts alone, and σ_{Ee} is the equivalent elastic buckling stress corresponding to the equivalent stress σ_e. It is natural to use the Von Mises stress,

$$\sigma_e = \sqrt{\sigma_x^2 + \sigma_y^2 - \sigma_x \sigma_y + \tau^2} \tag{3.19}$$

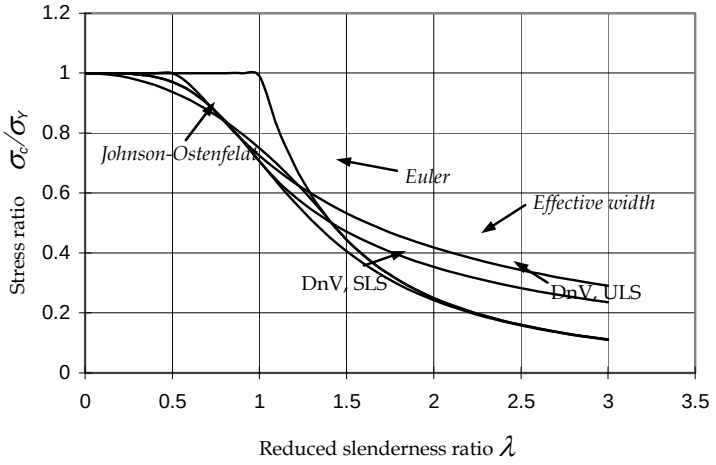

Figure 3.9 Elasto-Plastic Buckling Curves.

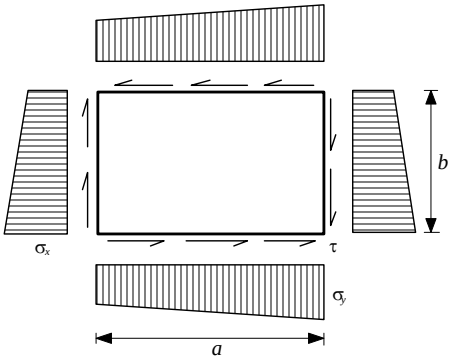

Figure 3.10 Combined Loading.

The equivalent reduced slenderness ratio to be used in the above modification for plasticity can then be expressed as,

$$\overline{\lambda}_e^2 = \frac{\sigma_Y}{\sigma_{Ee}} = \frac{\sigma_Y}{\sigma_e}\left[\left(\frac{\sigma_x}{\sigma_{Ex}}\right)^c + \left(\frac{\sigma_y}{\sigma_{Ey}}\right)^c + \left(\frac{\tau}{\tau_E}\right)^c\right]^{\frac{1}{c}} \tag{3.20}$$

The exponent c depends on the plate aspect ratio. Square plates tend to be more sensitive to combined loading than long plates, because the two buckling modes coincide for bi-axial compression. Therefore, a linear interaction is often used for square plates and an elliptic interaction for long plates. DNV classification note 30.1 specifies the following relationship,

$$c = 2 - \frac{1}{a/b} \quad , a/b > 1 \tag{3.21}$$

The above design procedure is intended for checks in the serviceability limit state (SLS). In most cases, plate buckling does not represent the ultimate capacity of the plate. If buckling does not represent a serviceability problem, for example excessive deformation for practical use of the structure or low cycle fatigue by repeated buckling and straightening of the plate, the ultimate capacity may be taken as

$$\sigma_{ult} = \frac{\sigma_Y}{\bar{\lambda}\sqrt{2}} \quad , 1.0 < \bar{\lambda} \le 5.0 \tag{3.22}$$

The two criteria are compared in Figure 3.11. For very slender plates the ultimate strength is significantly larger than buckling strength.

The post-buckling strength reserves are also utilized in the design of plate/stiffener as described in the subsequent sections.

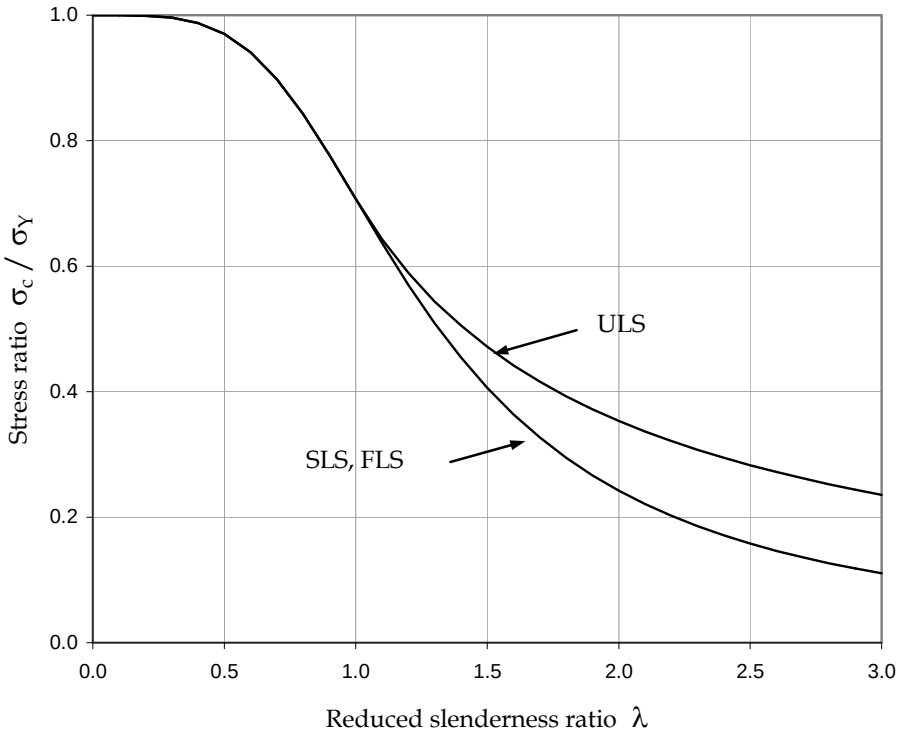

Figure 3.11 Ultimate Strength versus Buckling Strength Of Plates.

3.3 Post-Buckling Capacity of Plates

3.3.1 Effective Width Concept

Slender plates can carry load substantially in excess of what is predicted by elastic theory provided that their unloaded edges are constrained to remain straight. As a result of large lateral deflections, membrane stresses developes in the transverse direction, which tends to stabilize the plates. At this stage the distribution of stresses along the unloaded edges is no longer uniform but increases towards the stiffeners. According to the effective width method the ultimate load is obtained when the edge stress, σ_e, in Figure 3.12, approaches the yield stress. The following formula has been proposed for simply supported plates where the unloaded edges are constrained to remain straight, (reference /3/).

$$\frac{b_e}{b} = \frac{\sigma_{xm}}{\sigma_y} = \begin{cases} \frac{2}{\beta} - \frac{1}{\beta^2} \beta \geq 1 \\ 1 \beta \leq 1 \end{cases} \tag{3.23}$$

where the plate slenderness parameter is given by,

$$\beta = \frac{b}{t}\sqrt{\frac{\sigma_Y}{E}} \tag{3.24}$$

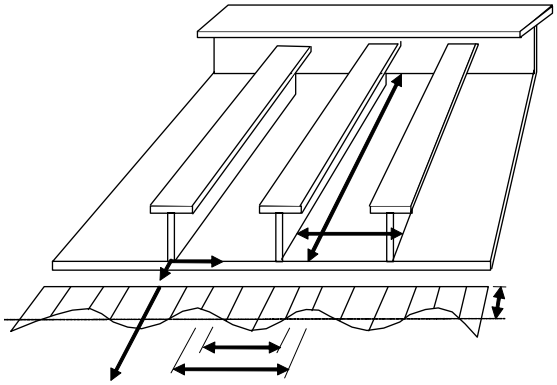

Figure 3.12 Actual Stress Distribution in a Compressed Stiffened Plate.

Equation (3.23) accounts for a reasonable degree of initial deflection in the buckling mode ($d_o/t \sim b^2/25$) but not residual stresses. The expression is plotted in Figure 3.9. It appears that the effective width formula predicts a considerable post-buckling reserve strength for slender plates. However, this additional capacity is reduced considerably if residual stresses are taken into account (see Section 3.3.4).

The post-buckling strength is normally not taken into account when designing plates for ships and offshore structures, since this would lead to flutter the plate each time the buckling load is exceeded. This is an undesired effect. However, in the analysis of combined stiffener-plate failure, the effective plate flange is often assessed by means of Equation (3.23), (see Section 3.4.2).

The expressions above hold true for a plate loaded on its short edge *b*. For compressive loads on the long edge, *a*, the following effective width formula has been proposed /4/.

$$\frac{a_e}{a} = \frac{\sigma_{ym}}{\sigma_Y} = \frac{0.9}{\beta^2} + \frac{1.9}{\alpha\beta}\left(1 - \frac{0.9}{\beta}\right) \quad , \quad \alpha = \frac{a}{b} \tag{3.25}$$

3.3.2 The Influence of Boundary Conditions

The actual boundary conditions will in most cases differ from the idealized cases shown in Figure 3.8. It is in generally accepted that the boundary conditions of the loaded edges do not have a significant influence on the ultimate strength and it is usual to model these edges as simply supported.

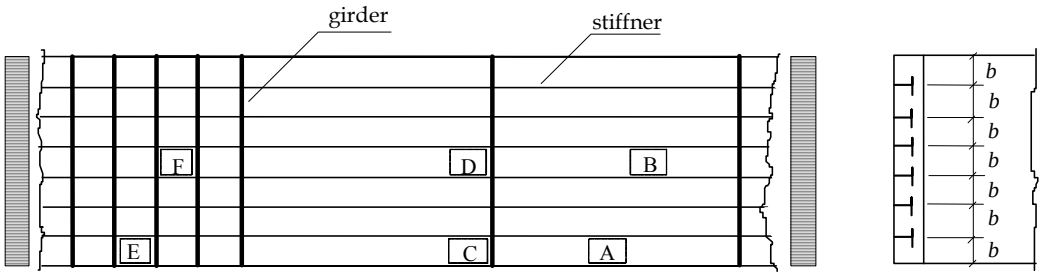

Figure 3.13 Various Boundary Conditions for Plate Elements in a Stiffened Panel.

The major influence stems form the conditions at the unloaded edges. These are dependent on the actual location of the plate field in the panel. With reference to Figure 3.13, plate F can be considered as restrained, plate B as constrained, and plate A as unrestrained. In the restrained case the edges remain undistorted while in the constrained case transverse displacements are allowed but the edges are forced to remain straight. In the unrestrained case the edges are completely free with respect to transverse displacement. The difference in boundary conditions, between plates B and F, is caused by the aspect ratio. The closeness of the transverse girders at F does not allow transverse displacements, while that may easily occur at the mid-section of plate B.

Generally, some degree of elastic rotational- and transverse restraint on the plate from the adjacent stiffeners are present. Their effect depends on the relation between stiffener dimensions and plate thickness. Results from numerical and experimental studies have shown that in-plane restraint can have a strengthening effect of 5-15%, depending on the plate slenderness and the magnitude of initial imperfections. The effect is more pronounced for slender plates and intermediate values of imperfections, δ_0, (see Figure 3.14). The rotational restraint shows a somewhat stronger influence, with a strengthening effect of 10-15%.

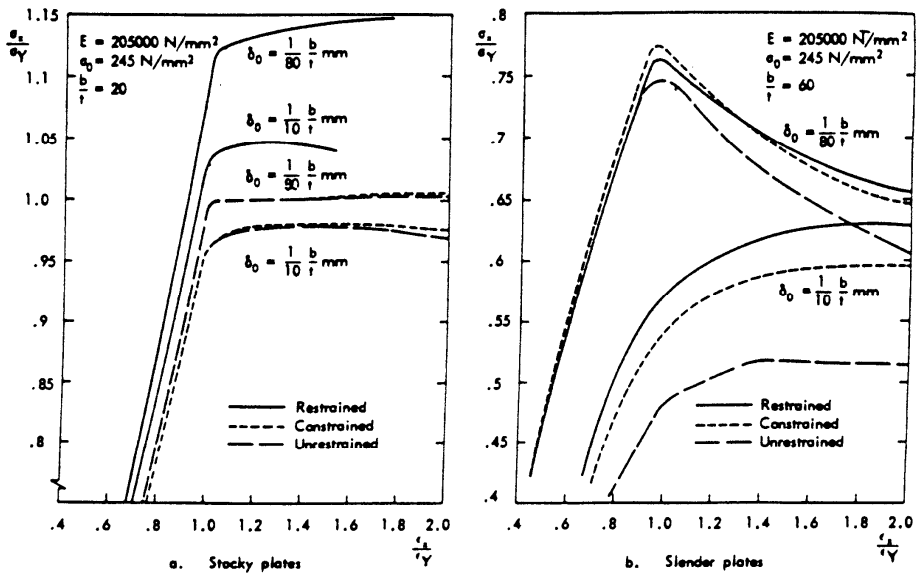

Figure 3.14 Effect of In-Plane Restraint on Plates in Compression.

3.3.3 The Influence of Initial Deflections

The effect of imperfections on the ultimate strength of plates depends strongly on their shape. In most theoretical studies, initial deflections have been assumed to have the same shape as the buckling mode which gives a reduction in ultimate stress. However, the welding process normally introduces an overall cylindrical deflection. This out-of-mode deflection may have a stiffening effect on plates as shown in Figure 3.15. However, this increase in ultimate strength is of little practical use since it is followed by a more violent nature of unloading.

It has been claimed that only the Fourier component of the deflected shape which coincides with the buckling mode has a significant influence on the ultimate strength as illustrated in Figure 3.16, (reference /6/). Statistical analysis of measurements of plate distortions shows that the amplitude of the buckling component is about half of the maximum distortions.

Various formulas are available for predicting the maximum distortion. The following relation has been used,

$$\frac{\delta_o}{t} = C_2 \frac{b}{t} - C_3 \qquad , \quad \frac{b}{t} > 40 \tag{3.26}$$

where, as proposed by Carlsen and Czujko /6/, $C_2 = 0.016$ and $C_3 = 0.36$.

The reduction in ultimate strength has been found to be almost linearly dependent on the magnitude of initial distortions /6/ but more sophisticated formulas also exist /7/.

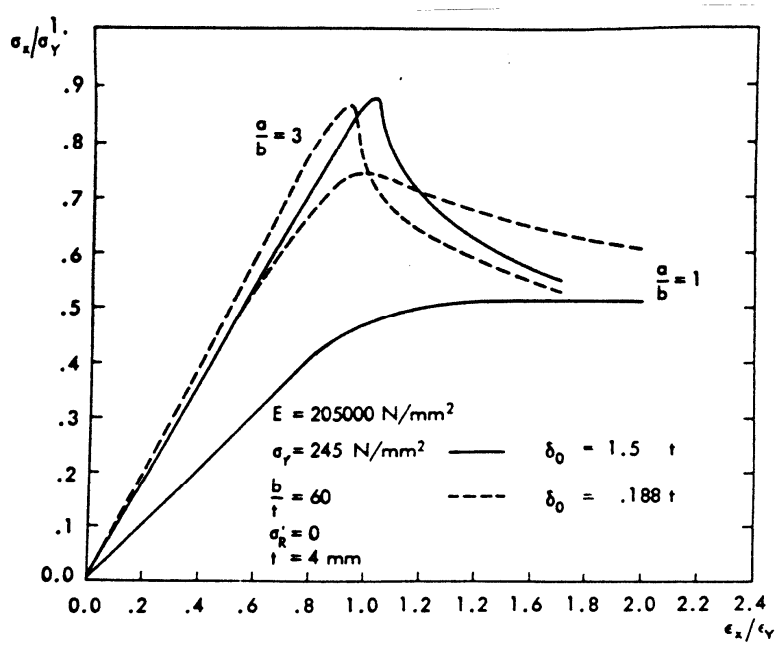

Figure 3.15 Load-End Shortening Curve for Rectangular and Quadratic Plate with Single Half-Sine-Wave Initial Imperfection; Edges Restrained.

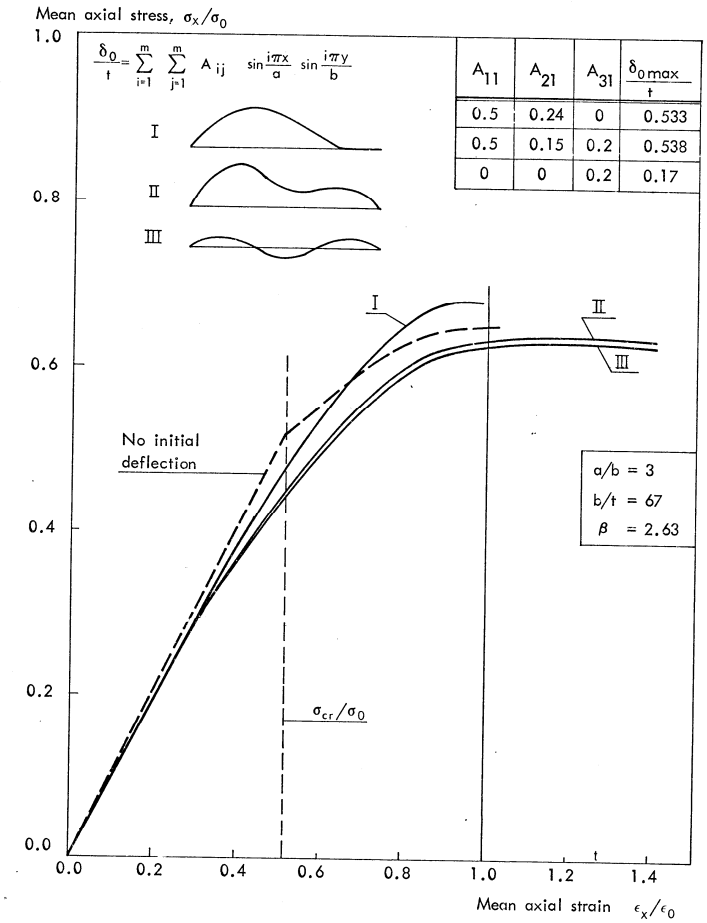

Figure 3.16 The Effect of Buckling Mode Components on Plate Strength /6/.

3.3.4 The Influence of Residual Stresses

The weld induced residual stress pattern in a stiffened panel is shown in Figure 3.17 (see also Section 1.2). The analysis model consists of a tension block in yield at the stiffener attachment which is balanced by a zone of uniform compressive residual stresses in the centre of the plate. The magnitude of these residual stresses results from equilibrium considerations.

$$\frac{\sigma_r}{\sigma_Y} = \frac{2\eta}{\frac{b}{t} - 2\eta} \tag{3.27}$$

A wide interval of η-values has been quoted. For as-welded structures, η tends to be very high. However, if the member is subject to alternating loads the residual stresses will be reduced after some years in service due to shake-out by occasional tension loads. Faulkner /3/, has suggested design values of η between 3 and 4.5 for actual ships.

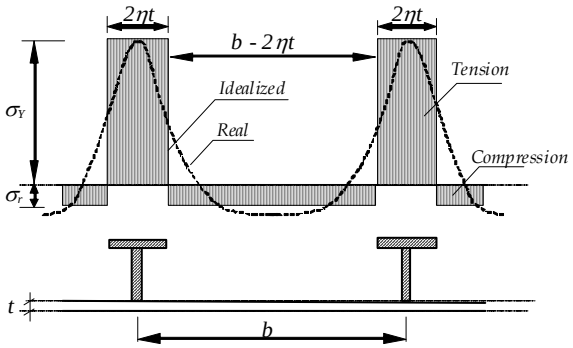

Figure 3.17 Welding Stress Pattern in Plates.

The effect of residual stresses is to cause loss of compressive plate stiffness as a result of premature yielding in the compression zone. The greatest sensitivity to residual stresses is in the region where

$\sigma_{cr} \cong \sigma_Y$, which happens for b/t ratio about 50-60, and is associated in a shift of compressive strain ε_u at failure from $\varepsilon_u < \varepsilon_Y$ for plates containing moderate residual stresses to $\varepsilon_u \cong 2\varepsilon_Y$ for plates with substantial residual stresses.

$$R_r = 1 - \frac{\sigma_r}{\sigma_Y}\frac{E_t}{E} = 1 - \frac{2\eta}{\frac{b}{t} - 2\eta}\frac{2(\beta - 1)}{\beta}, 1 < \beta < 2.5 \tag{3.28}$$

where E_t is the tangent modulus of the plate. The reduction in ultimate strength due to residual stresses can be calculated by multiplying the expression in Equation (3.23) with the factor given in Equation (3.28). For design purposes, the following simple expression, accounting for both reasonable initial deformations and residual stresses, is adopted in DNV Classification Note 30.1.

$$\begin{aligned} &\frac{b_e}{b} = \frac{\sigma_{xu}}{\sigma_Y} = \frac{1.8}{\beta} - \frac{0.8}{\beta^2} \qquad \beta \geq 1 \\ &\frac{b_e}{b} = 1 \qquad \beta \leq 1 \end{aligned} \tag{3.29}$$

3.3.5 Simple model for post-buckling capacity

Plates loaded into the post-buckling region can carry loads substantially in excess of the classical buckling load. This is because in-plane membrane forces develop in the transverse

direction at finite deflections. In order to illustrate this a simple is established. Consider the simply, supported square plate in Figure 3.18

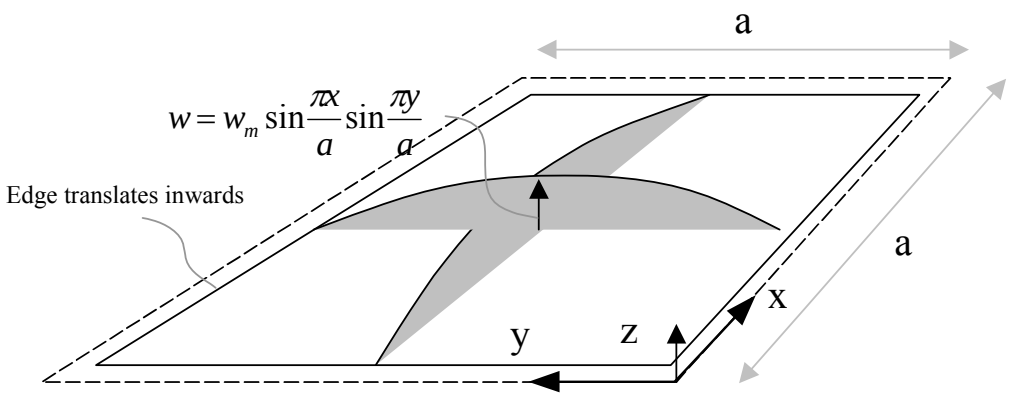

Figure 3.18 Assumed displacement function in the post-buckling range

During compression and buckling it is assumed that unloaded edges remain straight, but can translate inwards, i.e. constrained boundary conditions.

In the post-buckling range it is assumed that the total load-carrying capacity contains two terms:

1) The classical buckling load, which remains constant during finite deflections. For a square plate the stress is given by:

$$\sigma_E = \frac{\pi^2 E}{12\left(1-\nu^2\right)}\left(\frac{t}{a}\right)^2 4 \tag{3.30}$$

2) An additional stress $\Delta\sigma$ induced by membrane stresses in the transverse direction. This stress is non-uniform over the width of the plate.

The calculation of the additional stress is based upon the energy method. The following displacement function is assumed

$$w = w_m \sin\frac{\pi x}{a}\sin\frac{\pi y}{a} \tag{3.31}$$

$$w_{,y} = w_m \sin\frac{\pi x}{a}\left(\frac{\pi}{a}\right)\cos\frac{\pi y}{a} \tag{3.32}$$

This is exact solution at initiation of buckling and is assumed to describe the displacement in the post-critical range well.

The axial membrane strain for a plate strip in the transverse direction is given by

$$\varepsilon_y(x,y) = v_{,y} + \frac{1}{2} w_{,y}{}^2 \tag{3.33}$$

and the average strain becomes

$$\begin{aligned}
\varepsilon_{y,av}(x) &= \frac{1}{a}\int_0^a \left(v_{,y} + \frac{1}{2} w_{,y}^2 \right) dy \\
&= \frac{1}{a}\left(\Delta v + \frac{1}{2} w_m^2 \sin^2 \frac{\pi x}{a} \left(\frac{\pi}{a} \right)^2 \int_0^a \cos^2 \frac{\pi y}{a} dy \right) \\
&= \frac{\Delta v}{a} + \left(\frac{\pi w_m}{2a} \right)^2 \frac{1 - \cos \dfrac{2\pi x}{a}}{2}
\end{aligned} \tag{3.34}$$

Δv represents the transverse displacement of the unloaded plate edge. Since it remains straight Δv is constant. The average strain in transverse direction over the whole plate is given by

$$\bar{\varepsilon}_y = \frac{1}{a}\int_0^a \varepsilon_{y,av}(x) dx = \frac{\Delta \mathrm{v}}{\mathrm{a}} + \left(\frac{\pi w_m}{2a} \right)^2 \frac{1}{2} \tag{3.35}$$

With unconstrained edges the resultant force and hence the average strain should be equal to zero. This means that the unloaded edge translates inward a distance

$$\frac{\Delta v}{a} = -\frac{1}{2}\left(\frac{\pi w_m}{2a} \right)^2 \tag{3.36}$$

The resulting membrane strain is therefore

$$\varepsilon_{y,av} = \left(\frac{\pi w_m}{2a} \right)^2 \frac{-\cos \dfrac{2\pi x}{a}}{2} \tag{3.37}$$

To this strain there is associated a transverse membrane force given by

$$\Delta N_y = E\varepsilon_y t = Et\left(\frac{\pi w_m}{2a} \right)^2 \left(-\frac{\cos \dfrac{2\pi x}{a}}{2} \right) \tag{3.38}$$

The corresponding strain energy in the transverse direction is given by

$$U_m = \frac{1}{2}\int_0^a \int_0^a N_y(y)\varepsilon_{y,av}\,dxdy = \frac{a}{8}Et\left(\frac{\pi w_m}{2a}\right)^4 \int_0^a \cos^2\left(\frac{2\pi x}{a}\right)dx = \frac{a^2}{16}Et\left(\frac{\pi w_m}{2a}\right)^4 \tag{3.39}$$

The potential of the additional external load in x-direction is

$$H_{\Delta N x} = \frac{\Delta N_x}{2}\int_0^a \int_0^a w_{,x}{}^2\,dxdy = \frac{\Delta N}{8}\left(\frac{\pi w_m}{a}\right)^2 a^2 \tag{3.40}$$

(Note: The potential of external load is negative since ΔN_x is defined negative in compression)

The potential energy becomes

$$\Pi_{\Delta N_y} = U_m + H_{\Delta N_x} \tag{3.41}$$

The additional stress is determined from the condition

$$\delta(U_m + H_{\Delta N_x}) = 0 \tag{3.42}$$

or

$$\frac{a^2}{16}Et \cdot 4\left(\frac{\pi w_m}{2a}\right)^3 . \frac{\pi}{2a} + \frac{\Delta N_x}{8} \cdot 2\left(\frac{\pi w_m}{a}\right) . \frac{\pi}{a} a^2 = 0 \tag{3.43}$$

This yields

$$\Delta N_x = -Et\frac{\pi^2}{16}\left(\frac{w_m}{a}\right)^2 \tag{3.44}$$

Analogous to the calculation of strains in transverse direction the average membrane strain in the longitudinal direction can be written as

$$\bar{\varepsilon}_x = \frac{\Delta u}{\mathrm{a}} + \left(\frac{\pi w_m}{2a}\right)^2 \frac{1}{2} \tag{3.45}$$

In this case the following condition applies

$$\Delta N_x = Et\bar{\varepsilon}_x = Et\left(\frac{\Delta u}{a} + \left(\frac{\pi w_m}{2a}\right)^2 \frac{1}{2}\right) = -Et\frac{\pi^2}{4}\left(\frac{w_m}{2a}\right)^2 \tag{3.46}$$

This yields

$$\frac{\Delta u}{a} = -\frac{3}{4}\left(\frac{\pi w_m}{2a}\right)^2 \tag{3.47}$$

Hence the variation in y-direction of the additional stress resultant is given by

$$\Delta\sigma_x(y) = \frac{\Delta N_x(y)}{t} = Et\left(\frac{\Delta u}{a} + \left(\frac{\pi w_m}{2a}\right)^2 \frac{1-\cos\frac{2\pi y}{a}}{2}\right) \qquad (3.48)$$
$$= -Et\frac{\pi 2}{16}\left(\frac{w_m}{a}\right)^2\left\{1+2\cos\frac{2\pi y}{a}\right\}$$

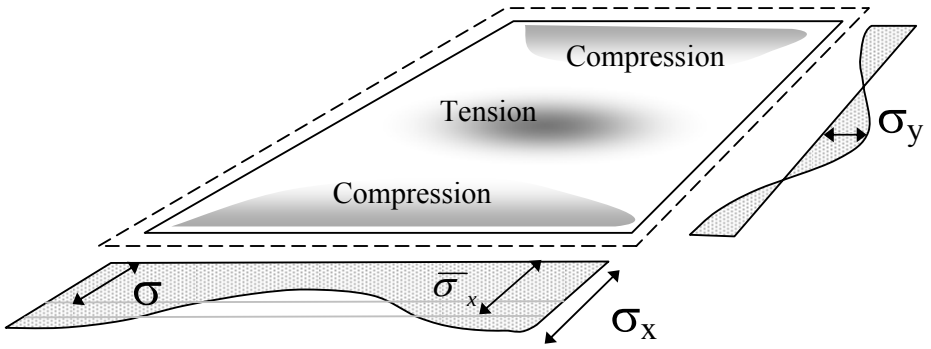

Figure 3.19 Stress distributions

This distribution is sketched in Figure 3.19 It is observed that the maximum compressive stress occurs at the boundaries while a stress relief is caused by the large displacements in the middle of the plate.

The maximum compressive stresses occurs along the unloaded edges (x = 0,a)

$$\sigma_x = -\sigma_E - E\frac{3\pi^2}{16}\left(\frac{w_m}{a}\right)^2 \qquad (3.49)$$

Along this edge, the stress in transverse direction varies between

$$\sigma_y = \pm E\frac{\pi^2}{8}\left(\frac{w_m}{a}\right)^2 \qquad (3.50)$$

Introducing the mean axial stress

$$\overline{\sigma}_x = -\sigma_E - \Delta\sigma = -\sigma_E - E\frac{\pi^2}{16}\left(\frac{w_m}{a}\right)^2 \qquad (3.51)$$

This can be written:

$$\sigma_x = -\sigma_E - 3(\overline{\sigma}_x - \sigma_E) = -\left(3\overline{\sigma}_x - 2\sigma_E\right)$$
$$\sigma_y = \pm 2(\overline{\sigma}_x - \sigma_E) \tag{3.52}$$

It may be assumed that the plate will fail once the von-Mises yield criterion is violated. The criterion reads

$$\sigma_x^2 - \sigma_x\sigma_y + \sigma_y^2 = \sigma_Y^2 \tag{3.53}$$

This means that the critical section will be in the middle of one of the unloaded edges where the longitudinal compressive stress and the transverse tensile stress attains a maximum

This yields

$$\left(3\overline{\sigma}_x - 2\sigma_E\right)^2 + (3\overline{\sigma}_x - 2\sigma_E)2(\overline{\sigma}_x - \sigma_E) + 4(\overline{\sigma}_x - \sigma_E)^2 = \sigma_Y{}^2 \tag{3.54}$$

This expression can be solved with respect to $\overline{\sigma}_x / \sigma_y$ yielding

$$\frac{\overline{\sigma}_x}{\sigma_Y} = \left(\frac{30}{\overline{\lambda}^2} + \sqrt{76 - \frac{12}{\overline{\lambda}^4}}\right)/38 \tag{3.55}$$

where the reduced slenderness is given by

$$\overline{\lambda} = \sqrt{\frac{\sigma_Y}{\sigma_E}} = 1.9\beta \tag{3.56}$$

The post-buckling stress is plotted versus the plate slenderness factor in Figure 3.20.

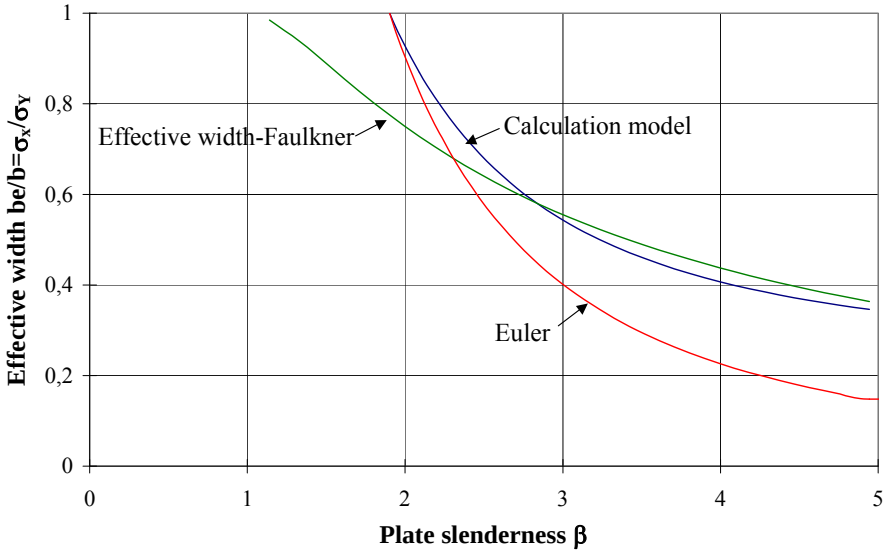

Figure 3.20 Effective width versus plate slenderness

It is observed that the simple calculation model yields a critical stress which is significantly higher than the Euler stress for slender plates. The model agrees very well with the formula proposed by Faulkner for high plate slenderness, but becomes too optimistic for low slenderness.

The reason for this discrepancy is the influence of initial deflections, which will cause yielding at lower load levels. Initial deflection may be taken into account in the simple model. We will then have to subtract the initial strain free condition in the expression for the axial strain, i.e.

$$\begin{aligned}\varepsilon_{y,av}(y) &= \frac{1}{a}\int_0^a \left(v_{,y} + \frac{1}{2}\left(w_{,y}^2 - w_{o,y}\right)\right)dx^2 \\ &= \frac{\Delta v}{a} + \left(\frac{\pi w_m - w_{om}}{2a}\right)^2 \frac{1-\cos\frac{2\pi x}{a}}{2}\end{aligned} \tag{3.57}$$

This implies that the strain energy now takes the form

$$U_m = \frac{a^2}{16} Et\left(\left(\frac{\pi w_m}{2a}\right)^2 - \left(\frac{\pi w_{0m}}{2a}\right)^2\right)^2 \tag{3.58}$$

The potential of the additional external load in x-direction is also affected by the initial deflection;

$$H_{\Delta N_x} = \frac{\Delta N_x}{2}\int_0^a\int_0^a \left(w_{,x}{}^2 - w_{0,x}{}^2\right)dxdy = \frac{\Delta N}{8}\left(\left(\frac{\pi w_m}{a}\right)^2 - \left(\frac{\pi w_{0m}}{a}\right)^2\right)a^2 \tag{3.59}$$

By minimising the potential energy there is obtained

$$\frac{a^2}{16} Et \cdot 2\left(\left(\frac{\pi w_m}{2a}\right)^2 - \left(\frac{\pi w_{0m}}{2a}\right)^2\right)2\frac{\pi}{2a} + \frac{\Delta N_x}{8}\cdot 2\left(\frac{\pi w_m}{a}\right).\frac{\pi}{a}a^2 = 0 \tag{3.60}$$

This yields

$$\Delta N_x = -Et\frac{\pi^2}{16}\left(\left(\frac{w_m}{a}\right)^2 - \left(\frac{w_{0m}}{a}\right)^2\right) \tag{3.61}$$

The stress in the pre-buckling range is also affected by the initial deflection. Recalling Equation (4.22) the stress resultant can be written as

$$N = N_E\left(1 - \frac{w_{0m}}{w_m}\right) \tag{3.62}$$

The stresses along the unloaded edge in the longitudinal – and transverse direction read accordingly:

$$\sigma_x = -\sigma_E\left(1-\frac{w_{0m}}{w_m}\right)-E\frac{3\pi^2}{16}\left(\left(\frac{w_m}{a}\right)^2-\left(\frac{w_{0m}}{a}\right)^2\right) \tag{3.63}$$

$$\sigma_y = \pm E\frac{\pi^2}{8}\left(\left(\frac{w_m}{a}\right)^2-\left(\frac{w_{0m}}{a}\right)^2\right) \tag{3.64}$$

Introducing the mean axial stress

$$\overline{\sigma}_x = -\sigma_E-\Delta\sigma = -\sigma_E\left(1-\frac{w_{om}}{w_m}\right)-E\frac{\pi^2}{16}\left(\left(\frac{w_m}{a}\right)^2-\left(\frac{w_{0m}}{a}\right)^2\right) \tag{3.65}$$

we get:

$$\begin{aligned}\sigma_x &= -\sigma_E\left(1-\frac{w_{0m}}{w_m}\right)-3\left(\overline{\sigma}_x-\sigma_E\left(1-\frac{w_{0m}}{w_m}\right)\right)=-\left(3\overline{\sigma}_x-2\sigma_E\left(1-\frac{w_{0m}}{w_m}\right)\right)\\ \sigma_y &= \pm 2\left(\overline{\sigma}_x-\sigma_E\left(1-\frac{w_{0m}}{w_m}\right)\right)\end{aligned} \tag{3.66}$$

The von Mises yield criterion at the middle of the unloaded edges can now be formulated

$$\left(3\overline{\sigma}_x-2\sigma_E^{\,|}\right)^2+(3\overline{\sigma}_x-2\sigma_E^{\,|})2(\overline{\sigma}_x-\sigma_E^{\,1})+4(\overline{\sigma}_x-\sigma_E^{\,|})^2=\sigma_Y^{\,2} \tag{3.67}$$

where

$$\sigma_E^{\,|}=\sigma_E\left(1-\frac{w_{0m}}{w_m}\right) \tag{3.68}$$

The solution becomes:

$$\frac{\overline{\sigma}_x}{\sigma_Y}=\left(\frac{30\left(1-\frac{w_{0m}}{w_m}\right)}{\overline{\lambda}^2}+\sqrt{76-\frac{12\left(1-\frac{w_{0m}}{w_m}\right)^2}{\overline{\lambda}^4}}\right)/38 \tag{3.69}$$

Since we don't know a priori the magnitude of the deflection that satisfies the yield criterion, an iterative procedure is required in order to determine w_m.

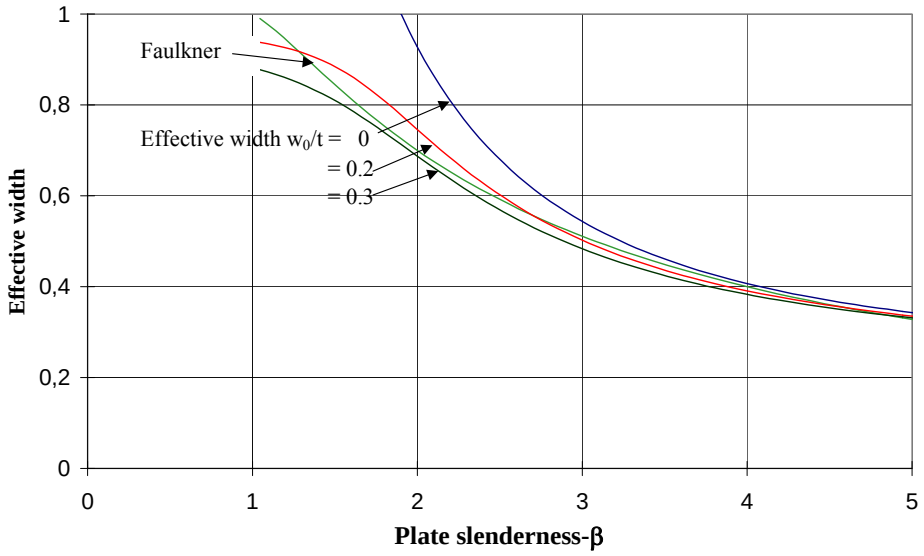

Figure 3.21 shows the effective width obtained with two different initial deflections. It appears that a deflection amplitude in the range of 0.2-0.3 times the plate thickness yields quite good agreement with Faulkner's expression except for small plate slenderness.

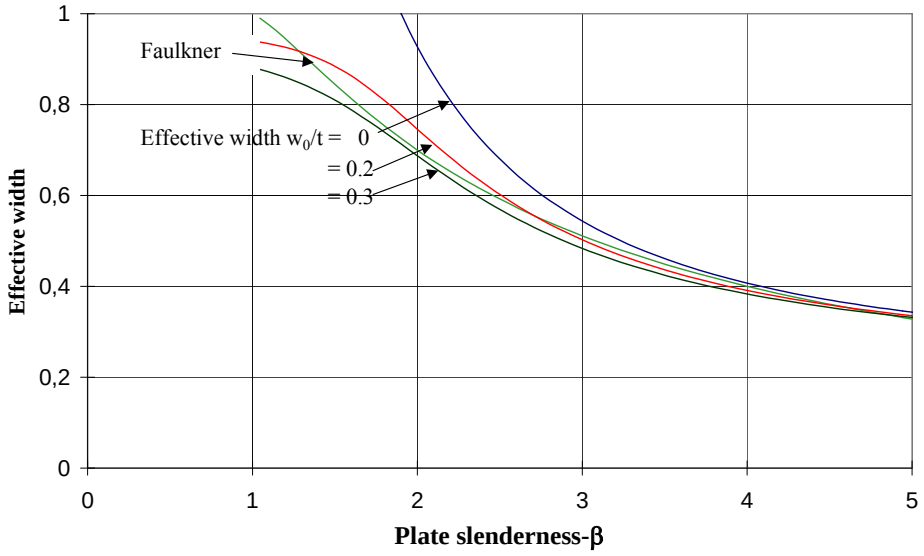

Figure 3.21 Effective width with initial deflection.

3.3.6 Marguerre's large deflection equations for plates

In order to study the post-buckling capacity of plates subjected to in-plate compression it is necessary to study the effect of large deflections.

In the subsequent analysis, plates which have an initial imperfection in the form of double sinusoidal wave will be studies, see Figure 3.22.

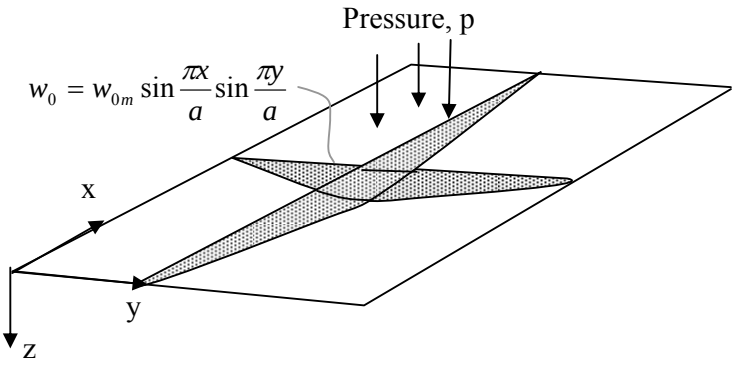

Figure 3.22 Plate with initial imperfection

Let us first consider what happens when a plate strip of length dx with an initial deflection change dw is further deformed as shown in Figure 3.23.

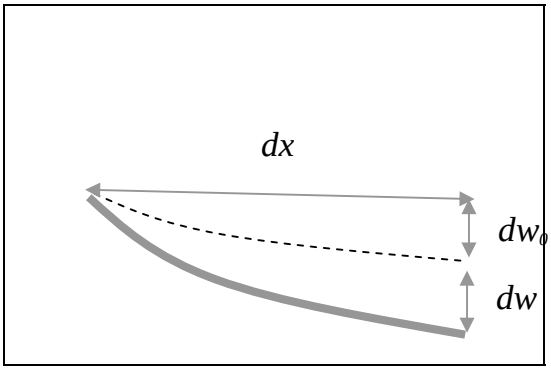

Figure 3.23 Deformed configuration of plate element

It is seen that plate stretches due to the deformation. The elongation is given by

$$d\ell = \sqrt{dx^2 + (dw_0 + dw)^2} - \sqrt{dx^2 + dw_0^2} \tag{3.70}$$

or

$$\begin{aligned} \frac{d\ell}{dx} &= \sqrt{1 + (w_{0,x} + w_{,x})^2} - \sqrt{1 + w_{0,x}^2} \\ &\approx 1 + \frac{1}{2}(w_{0,x} + w,x)^2 - (1 + \frac{1}{2} w_{0,x}^2) \\ &= w_{0,x} w_{,x} + \frac{1}{2} w_{,x}^2 \end{aligned} \tag{3.71}$$

The approximate relationship is obtained by a Taylor series expansion of the root expression and is valid for moderate rotations. It is natural to associate $\frac{d\ell}{dx}$ with a strain caused by lateral deflection. The total strain should also include the in-plate (linear) part so that there is obtained

$$\varepsilon_x = u_{,x} + w_{0,x}\, w_{,x} + \frac{1}{2} w_{,x}^{\,2} \tag{3.72}$$

Similarly in the y-direction

$$\varepsilon_y = v_y + w_{0,y}\, w_{,y} + \frac{1}{2} w_{,y}^{\,2} \tag{3.73}$$

The corresponding term for shear strain reads

$$\varepsilon_{xy} = \frac{1}{2} j_{xy} = \frac{1}{2}(u_{,y} + v_{,x} + w_{0,x}\, w_{,y} + w_{0,y}\, w_{,x} + w_{,x}\, w_{,y} \tag{3.74}$$

It is recalled (cfr. «Skiver og plater») that the compatibility requirement for a membrane element (in-plane loading) could be expressed as

$$\nabla^4 \Phi = -w_{o,xx}\, w_{,yy} + 2w_{0,xy}\, w_{,xy} - w_{0,yy}\, w_{,xx} + w_{,xy} - w_{,xx}\, w_{,yy} \tag{3.75}$$

where the stress function $\square$ has been introduced. It is related to the stresses by

$$N_x = \Phi_{,YY}\,,\; N_{xy} = -\Phi_{,xy}\,,\; N_y = \Phi_{,xx}$$

It is seen that the above equation specialises to the well-known disk equation $\nabla^4 \Phi = 0$ for no initial displacements and no lateral deformation.

The equilibrium equation in the lateral direction is given by

$$\begin{aligned} D\nabla^4 w &= \left[\Phi_{,yy}\,(w_{0,xx} + w_{,xx}) - 2\Phi_{,xy}\,(w_{0,xy} + w_{,xy}) + \Phi_{,xx}\,(w_{0,yy} + w_{,yy})\right] - p \\ &= 0 \end{aligned} \tag{3.76}$$

Equations 3.76 are called Marguerre's simultaneous non-linear partial differential equations for a plate subjected to combined in-plane and lateral loading.

They couple both the bending behaviour and the membrane behaviour for a plate undergoing finite deflections. The are quite general and cover both plates with initial deflection ($w_0 \neq 0$) and that plates $(w_0 = 0)$. In the latter case, if there is no lateral loading, i.e. p = 0 is specialises the well-known equation

$$D\nabla^4 w - \left[N_X\, w_{,xx} + 2N_{xy} w_{,xy} + N_y\, w_{,yy}\right] = 0 \tag{3.77}$$

3.3.7 The Influence of Combined Loading

The effect of hydrostatic loading is to produce a deflection of cylindrical shape between stiffeners. In simplified approaches, this is often treated as an additional initial deflection. However, the occurrence of lateral load on slender plates creates a non-linear behaviour, which does not necessarily reflect the performance of initially deflected plates. For example, tensile stresses caused by membrane carrying of the lateral load will be present at zero compressive load.

For square plates the initial deflection caused by lateral load is similar to the buckling mode and a reduction of compressive strength is normally observed. For long plates the buckling will take on a higher mode shape which leads to a strengthening effect. However, the post-collapse behaviour may be more violent.

The lateral pressure in ship structures are normally moderate. Since most ship plates are long, the effect of lateral load has normally been neglected in plate design.

As explained in Section 3.1, plate elements are sometimes subjected to a biaxial state of stress yielding a decrease in the unaxial load-carrying capacity. Various interaction type of formulas have been proposed on the basis of experimental and numerical studies. The following is due to Faulkner /4/.

$$\frac{\sigma_x}{\sigma_{xu}} + \left(\frac{\sigma_y}{\sigma_{yu}}\right)^2 = 1 \tag{3.78}$$

where σ_{xu} and σ_{yu} denote the uniaxial ultimate compressive stresse in the axial and transverse direction, respectively. An alternative interaction curve has been proposed by Valsgård /8/.

$$\frac{\sigma_x}{\sigma_{xu}} - 0.25\frac{\sigma_x}{\sigma_{xu}}\frac{\sigma_y}{\sigma_{yu}} + \left(\frac{\sigma_y}{\sigma_{yu}}\right)^2 = 1 \tag{3.79}$$

For the more complex type of loading involving bi-axial compression, and shear combined with in-plane bending, Harding and Dowling /9/ suggested

$$\sqrt{\left(\frac{\sigma_x}{\sigma_{xu}}\right)^2 + \left(\frac{\sigma_y}{\sigma_{yu}}\right)^2} + \left(\frac{\sigma_b}{\sigma_{bu}}\right)^2 + \left(\frac{\tau}{\tau_u}\right)^2 = 1 \tag{3.80}$$

It should be noted that for the case of pure bi-axial loading, Equation (3.80) represents still a different interaction formula.

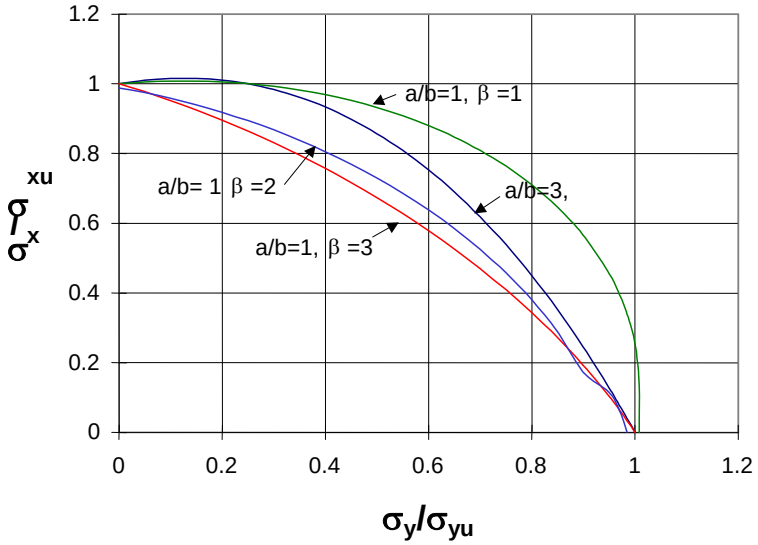

Figure 3.24 Interaction curve for bi-axial compression according to DnV Class.Note 30.1

Several of the interaction curves that have been proposed can be incorporated in the equation,

$$\left(\frac{\sigma'_{xu}}{\sigma_{xu}}\right)^{c_1} + c_2 \frac{\sigma'_{xu}}{\sigma_{xu}}\frac{\sigma_y}{\sigma_{yu}} + \left(\frac{\sigma_y}{\sigma_{yu}}\right)^2 = 1 \qquad (3.81)$$

where the coefficients c_1 and c_2 vary according to the plate aspect ratio. For long plates ($a/b > 3$), it seems reasonable to assume that $c_1 = 1$ and $c_2 = 0.25$ independent of the plate slenderness. For square plates, the interaction depends heavily on the slenderness ratio b. On the basis of curve fitting results of numerical studies, DNV classification note 30.1 specifies,

$$\begin{aligned} c_1 &= 2 \\ c_2 &= 3.2\, e^{-0.35\beta} - 2 \end{aligned} \qquad (3.82)$$

It is observed from Figure 3.24 that stocky plates are less influenced by bi-axial compression. The failure criterion approaches the von Mises yield criterion. Slender, square plates experiences a significant interaction. Long plates are much less influenced because the failure modes are not compatible.
Hence, the following reduction factors are obtained

$$\frac{\sigma'_{xu}}{\sigma_{xu}} = \frac{b'_e}{b_e} = \frac{1-\left(\frac{\sigma_y}{\sigma_{yu}}\right)^2}{1-0.25\left(\frac{\sigma_y}{\sigma_{yu}}\right)^2} \quad , a/b \geq 3$$

$$\frac{\sigma'_{xu}}{\sigma_{xu}} = \frac{b'_e}{b_e} = 0.5c_2\frac{\sigma_y}{\sigma_{yu}} + \sqrt{1-\left(1-0.25c_2^2\right)\left(\frac{\sigma_y}{\sigma_{yu}}\right)^2} \quad , a/b = 1 \qquad (3.83)$$

where,

$$\sigma_{yu} = \sigma_Y \frac{a_e}{a} \tag{3.84}$$

For intermediate values of the aspect ratio, interpolation is used. In the case that the plate is in tension in the *y*-direction, the ultimate strength in *y*-direction is equal to the yield stress, so that the following interaction is adopted,

$$\left(\frac{\sigma'_{xu}}{\sigma_{xu}}\right)^2 + \left(\frac{\sigma'_{xu}}{\sigma_{xu}}\right)\left(\frac{\sigma_y}{\sigma_Y}\right) + \left(\frac{\sigma_y}{\sigma_y}\right)^2 = 1 \tag{3.85}$$

Solving this yields,

$$\frac{\sigma'_{xu}}{\sigma_{xu}} = \frac{b'_e}{b_e} = \frac{1}{2}\left[\sqrt{4 - 3\left(\frac{\sigma_y}{\sigma_Y}\right)^2} - \frac{\sigma_y}{\sigma_Y}\right] \tag{3.86}$$

If the plate is subjected to shear, a further reduction is needed,

$$\left(\frac{\sigma''_{xu}}{\sigma'_{xu}}\right)^2 + \left(\frac{\sqrt{3}\tau}{\sigma_Y}\right)^2 = 1 \tag{3.87}$$

or,

$$\frac{\sigma''_{xu}}{\sigma'_{xu}} = \frac{b''_e}{b'_e} = \sqrt{1 - 3\left(\frac{\tau}{\sigma_y}\right)^2} \tag{3.88}$$

The total effective width factor is expressed as the product of the effective width in the *x*-direction and the respective modification for transverse stress and shear. This yields,

$$\frac{b''_e}{b} = \frac{b''_e}{b'_e}\frac{b'_e}{b_e}\frac{b_e}{b} \tag{3.89}$$

If the stiffener fails towards the plate, such that the plate bends in tension, the above formulas are too conservative. DNV specifies the following effective width formula,

$$\frac{b'_e}{b} = 1.1 - 0.1\beta \le 1 \ , \quad \text{(Tension)} \tag{3.90}$$

3.4 Buckling of Stiffened Plates

3.4.1 Collapse Modes

A stiffener with its associated plate flange is conveniently modelled as an equivalent beam-column as shown in Figure 3.25. The following main types of collapse are distinguished, (see Figure 3.26):-

i.) *Flexural buckling*;
- towards the stiffener, i.e. plate induced failure
- towards the plate, i.e. stiffener induced failure

ii.) *Tripping sideways of stiffener*.

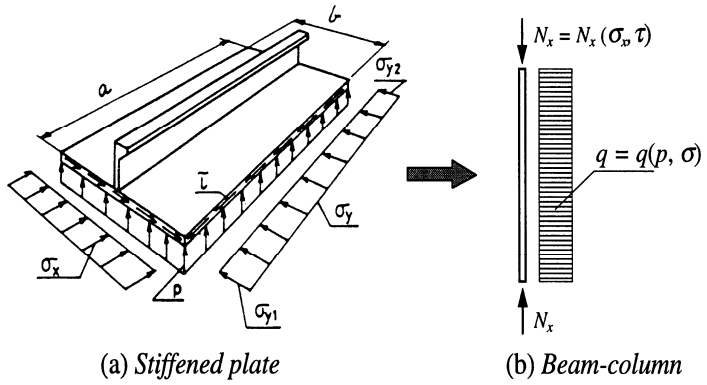

(a) *Stiffened plate* (b) *Beam-column*

Figure 3.25 Equivalent Beam-Column Model of a Stiffened Plate.

(a) *Plate induced.* (b) *Stiffener induced.* (c) *Tripping failure of stiffner.*

Figure 3.26 Interframe Collapse Modes in Stiffened Plates.

3.4.2 Ideal Elastic-Plastic Strut Analysis

An approximate solution for the collapse load is given by the intersection point of the load-deflection curves calculated for an ideal elastic column and a perfectly plastic column. The elastic load-deflection curve for a pinned beam-column with a sinusoidal initial deflection of amplitude δ_o was derived in Section 4.3,

$$\delta_e = \delta_o \left(1 - \frac{N}{N_E} \right)^{-1} \tag{3.91}$$

where N_E is the Euler buckling load. The perfectly plastic solution can be expressed as,

$$\delta_P = \frac{M}{N} \tag{3.92}$$

where the bending moment, M, and the axial force, N, must satisfy the plastic interaction curve of the cross-section. This depends on the direction of bending.

Consider the stiffener cross-section shown in Figure 3.27 where the effective plate flange area, A_e, is greater than the web area, A_W. It is assumed that the resultant axial force acts through the elastic neutral axis, G. For bending towards the plate, the plastic neutral axis is assumed to be at the intersection between the plate and the stiffener, which gives a linear interaction formula,

$$\frac{M}{M_P} + \frac{N}{N_P} = 1 \tag{3.93}$$

For bending towards the stiffener the interaction formula reads,

$$\frac{M}{M_P}+\frac{N}{N_P}-2\left(\frac{z}{h_w}\right)^2=1 \tag{3.94}$$

where the last term on the left hand side is defined in Figure 3.27. It appears that a small axial load is favourable with respect to the moment capacity.

The elastic solution, given by Equation (3.91), along with the plastic solution for bending towards the plate, Equations (3.91-92) are plotted in Figure 3.27. The collapse load, interpreted as the intersection between the two curves, are shown to agree well with results from finite element analysis.

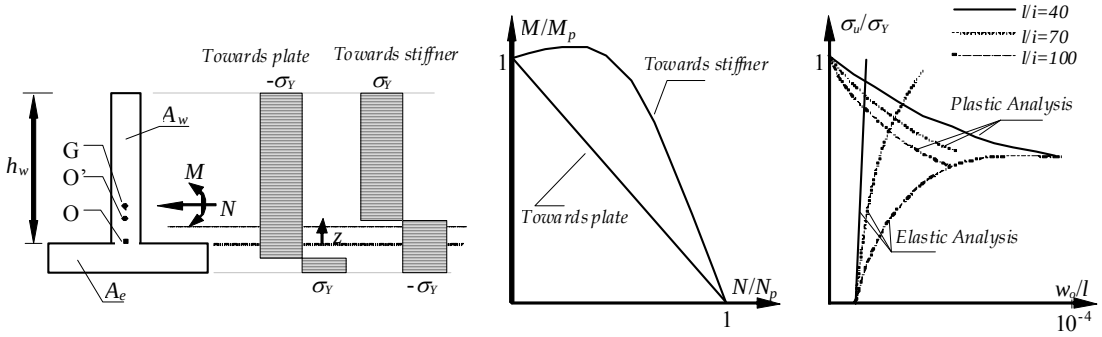

Figure 3.27 Elastic-Plastic Strut Analysis of Plate-Stiffener.

3.4.3 Effective Width Method According to Faulkner

This method, proposed by Faulkner /4/, is based on the elastic critical load for a strut with pinned ends,

$$\sigma_E=\frac{\pi^2 EI'_e}{l^2\left(A_w+A_e\right)} \tag{3.95}$$

modified for plasticity according to the Johnson-Ostenfield formulation, Equation (3.17)

$$\frac{\sigma_e}{\sigma_y}=1-\frac{\overline{\lambda}^2}{4} \qquad ,\overline{\lambda}^2\le 2 \tag{3.96}$$

The ultimate strength is reduced to account for loss of plate stiffness,

$$\sigma_u=\sigma_e\frac{A_w+A_e}{A_w+A_p} \tag{3.97}$$

The effective moment of inertia of the stiffener is calculated for a tangent (reduced) effective width of the plate given by,

$$\frac{b_e}{b}=\frac{1}{b}\sqrt{\frac{\sigma_y}{\sigma_e}} \tag{3.98}$$

where σ_e is the edge stress (Figure 3.12). The effective width of the plate is given by Equation (3.23) which accounts for initial deflections. The effective width should be reduced by the R_r, R_y, and R_τ, which represent, respectively, the effects of residual stresses, bi-axial loading, and shear stresses. R_r is given by Equation (3.28). From Equation (3.30) results,

$$R_y = 1 - \left(\frac{\sigma_y}{\sigma_{yu}} \right)^2 \quad \sigma_y \le 0.25\,\sigma_{yu} \tag{3.99}$$

and,

$$R_\tau = \sqrt{1 - \left(\frac{\tau}{\tau_y} \right)^2} \tag{3.100}$$

An iterative procedure is required for calculating the correct value of σ_e/σ_y, but usually few iterations are necessary.

In a comparative study carried out by Guedes Soares /1/, it is concluded that both simplified methods (Section 3.4.3; Effective width, and Section 3.4.5; Initial yield) predict the collapse load reasonably well. The consistency of the predictions is also good, showing coefficients of variation in the order of 10%. The initial yield method generally underpredicts the strength somehow. Hence, a safety margin is implicitly incorporated. However, this is not the case for the effective width method which should be used with explicit safety factors.

3.4.4 Interaction Between Compression and Lateral Pressure

For moderate lateral loads, the critical buckling mode will be the one with alternating buckling in the adjacent spans, and the buckling load is not influenced by the pressure of the lateral load. However, as the lateral load increases beyond a certain level, the buckling mode will shift to the one where all spans bow away from the pressure side. Failure is then plate-induced and the stiffeners may be assumed to be clamped. Conservatively, a linear interaction formula is used for this failure mode /10/.

$$\frac{\sigma_x}{\sigma_y} + \frac{q}{q_u} = 1 \tag{3.101}$$

where the rigid-plastic collapse load for a three-hinge beam mechanism for the stiffener is given by,

$$q_u = \frac{8\left(Z_t + Z_c\right)\sigma_y}{bl^2} \tag{3.102}$$

When calculating the section modulus of the stiffeners, Z_t and Z_c, account should be taken for the effective width of the plate flange in tension (Z_t) as well as in compression (Z_c).

3.4.5 Initial Yield Method (DNV Classification Note 30.1)

The buckling check in stiffened plates is based upon a beam column approach,

$$\frac{\sigma_x}{\sigma_{xcr}} + \frac{\sigma_b}{\left(1 - \frac{\sigma_x}{\sigma_E}\right)\sigma_Y} = 1 \tag{3.103}$$

where σ_x is the axial stress, σ_{xcr} is the critical stress for plate/stiffener in pure compression, σ_b is the design bending stress, σ_Y is the yield stress, and σ_E is the Euler buckling stress for plate/ stiffener.

The critical stress for pure compression is determined in the same way as described for columns, that is,

$$\frac{\sigma_{xcr}}{\sigma_Y} + \frac{\sigma_{xcr}}{1 - \frac{\sigma_{xcr}}{\sigma_E}} \frac{w_{eq} A}{\sigma_Y W} = 1 \tag{3.104}$$

where, $w_{eq} = 0.0015l$, is an equivalent imperfection accounting for the true out-of-straightness and the effect of fabrication stresses, and l is the member length. Introducing the factor,

$$\mu = \frac{w_{eq} A}{W} = 0.0015 l \frac{z}{i^2} \tag{3.105}$$

where z is the distance from the neutral axis to the stress point in question, the critical axial stress comes out to be,

$$\frac{\sigma_{xcr}}{\sigma_Y} = \frac{1 + \mu + \overline{\lambda}^2 - \sqrt{\left(1 + \mu + \overline{\lambda}^2\right)^2 - 4\overline{\lambda}^2}}{2\overline{\lambda}^2} \tag{3.106}$$

where the reduced slenderness is defined by,

$$\overline{\lambda} = \sqrt{\frac{\sigma_Y}{\sigma_E}} \quad , \quad \sigma_E = \frac{\pi^2 E i_e^2}{l_e^2} \tag{3.107}$$

The effective radius of gyration is defined by,

$$i_e = \sqrt{\frac{I_e}{A + b_e t}} \tag{3.108}$$

The effective moment of inertia can be written as,

$$I_e = I + e^2 A \left(1 + \frac{A}{b_e t}\right)^{-1} \tag{3.109}$$

where e is the eccentricity of the stiffener (without plate flange) to the plate flange, (confer Figure 3.28), I is the moment of inertia of the stiffener without plate flange, b_e is the effective width of the plating calculated as described in Section 3.3.5, and t is the plate thickness.

For plate induced failure there is a shift of the neutral axis due to loss of effective width. This causes an extra eccentricity for the plate/stiffener which has to be taken into account. This is illustrated in Figure 3.28.

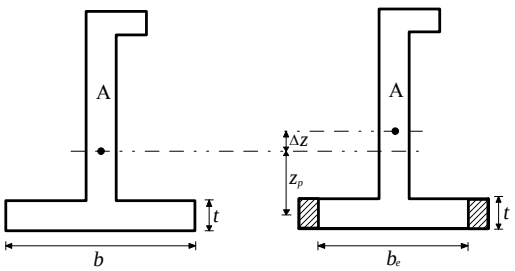

Figure 3.28 Shift of Effective Neutral Axis After Plate Buckling.

The shift of neutral axis comes out to be,

$$\Delta z = z_p \frac{(b - b_e)t}{A + bt} = z_p \left(1 - \frac{A + b_e t}{A + bt}\right) \tag{3.110}$$

where z_p is the distance from the plate flange to the original neutral axis. This shift of neutral axis has to be added to the equivalent initial imperfection used to calculate the ultimate capacity if the plate/stiffener, yielding

$$w_{eq} = 0.0015l + \Delta z \tag{3.111}$$

In the DNV Classification Note 30.1, two factors are introduced in order to get better agreement between the simple design formulas and numerical simulations. The initial distortion is magnified by a factor of 2.25 for stiffener induced failure, and Δz is reduced by 0.65 for plate induced failure.

The effective buckling length depends on the lateral pressure. If lateral pressure is not present, it is natural to assume that the effective length is equal to the stiffener span (frame spacing). When lateral pressure is present two failure modes can be envisaged:-

- asymmetric buckling with respect to the frame (*in-out*), i.e. the pressure is not sufficiently large to enforce buckling deformations to one side,
- symmetric buckling with respect to the frame.

Generally, the over-pressure may be on either the plate side or the stiffener side. This yields four potential buckling modes as shown in Figure 3.29.

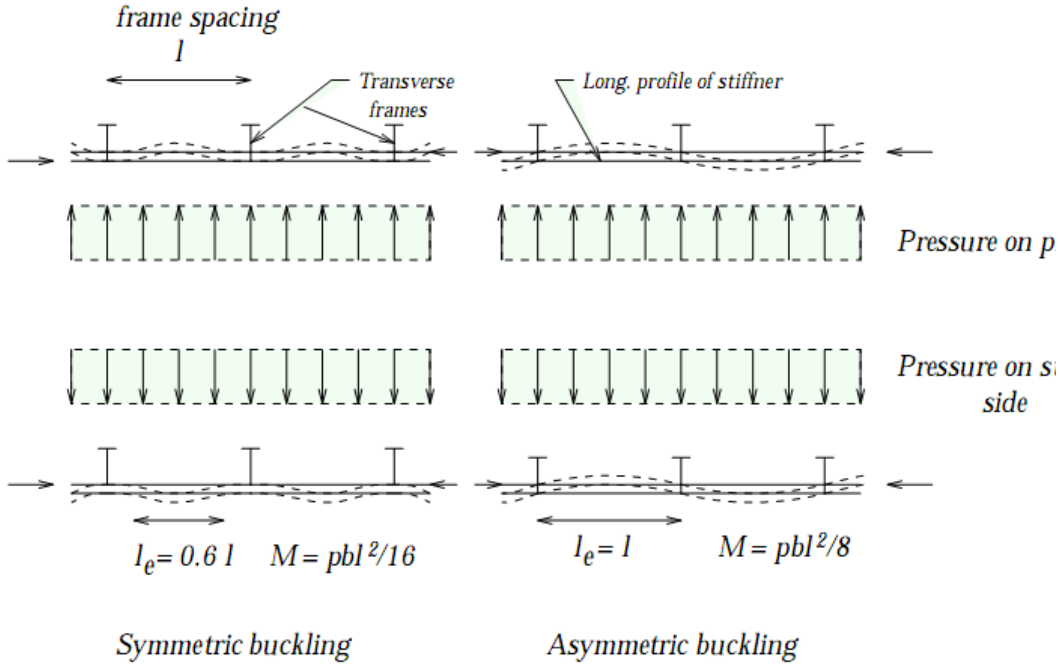

Figure 3.29 Potential Buckling Modes for Plate/Stiffener.

If the lateral pressure is large, the stiffener buckles symmetrically with respect to the frame. This is modelled as clamped end conditions. The corresponding buckling length is theoretically 0.5*l*. In the DNV Classification Note 30.1, the effective buckling length is somewhat conservatively set to 0.6l. The bending moment and the corresponding stress is calculated from a mechanism approach,

$$\sigma_b = \frac{1}{16}\frac{qbl^2}{W} \tag{3.112}$$

where *W*, the elastic section modulus, should be calculated with the effective plate flange and evaluated with respect to the plate flange or the stiffener top (stiffener induced failure).
If the hydrostatic pressure is not large enough, the stiffener buckles asymmetrically with respect to the frame. In this case, simply supported boundary conditions are more relevant and the bending stress is given by

$$\sigma_b = \frac{1}{8}\frac{qbl^2}{W} \tag{3.113}$$

The effective buckling length is equal to the stiffener span.

In addition to the buckling check on the compressive side, the tensile side of the plate/stiffener must be checked with respect to yielding given by the expression,

$$-\frac{\sigma_x}{\sigma_Y} + \frac{\sigma_b}{\left(1-\frac{\sigma_x}{\sigma_E}\right)\sigma_Y} = \eta \tag{3.114}$$

where η is the allowable usage factor. (Note that the bending stress is evaluated on the tensile side of the plate stiffener).

The characteristic material strength is equal to the yield stress for plate induced failure. For stiffener induced failure possible interaction with restrained torsional buckling has to be taken into account. Hence, the characteristic material strength is taken as the smaller of the yield stress and the torsional buckling stress.

In conclusion, the lateral pressure on plate side must be performed checked.

3.4.6 Buckling of Stiffeners and Girders according to NORSOK N-004/DnV RPC201

Equivalent load effects

The plate stiffener is modeled as a beam-column subjected to equivalent axial force and a lateral line load as shown in Figure 3.30.

The equivalent axial force is the actual axial force plus a tension field action (refer Chapter 4). The tension field concept allows shear stresses to develop beyond the stress level for plate

shear buckling between *stiffener* and *girders*, τ_{crl}. This shear stress is carried by tension forces between the stiffeners as illustrated by the shaded areas in Figure 3.31 . The additional shear force which must be carried by compression of the stiffener is calculated as:

$$N_\tau = \left(\tau - \tau_{crg}\right) st \qquad \textbf{(3.115)}$$

Where τ_{crg} is the critical shear stress between the girders, i.e. when the stiffeners are removed. The reason that $\tau_{crg} < \tau_{crlr}$ must be used is that the plate in the post-buckled state can only be assumed to carry the shear force between the girders alone.

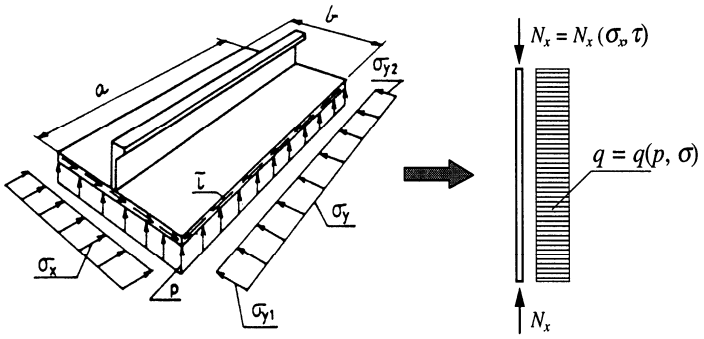

(a) *Stiffened plate* (b) *Beam-column*

Figure 3.30 Equivalent beam-column model of stiffened plate

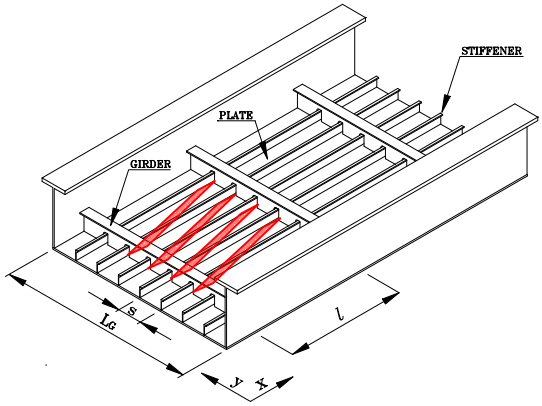

Figure 3.31Tension field in stiffened plate

Also the transverse stresses, σ_y, are considered to have a driving effect on plate/stiffener buckling. This is modeled as an equivalent lateral pressure, $p_{\sigma y}$.

The buckling stress of a transversely stiffened plate is given by(refer Eq. 3.125) (b =ℓ,a =L_g)

$$\sigma_{yE} = \frac{\pi^2 D}{\ell^2 t}\left[\left(\frac{m\ell}{L_G} + \frac{L_G}{m\ell}\right)^2 + i_s\left(\frac{L_G}{m\ell}\right)^2\right] \qquad (3.116)$$

where i_s is the smeared stiffness of the stiffener normalised versus the plate bending stiffness.

Minimising the buckling stress there is obtained

$$\sigma_{yE} = \frac{\pi^2 D}{\ell^2 t} 2\left(1 + \sqrt{1 + \frac{I_s / s}{t^3 / 12(1-\nu^2)}}\right) \qquad (3.117)$$

The maximum bending stress in a continuous stiffener subjected to uniform pressure occurs in the top flange and is given by:

$$\sigma_b = \frac{ps\ell^2}{12W_s} \tag{3.118}$$

where W_s is the section modulus of the stiffener with effective plate flange. Conversely,

$$p = \frac{12W_s\sigma_b}{\ell^2 s} \tag{3.119}$$

The equivalent bending stress to is scaled such that it attains the yield stress, σ_Y when the transverse stress σ_y equals the Euler buckling stress σ_{yE}. (Hence, for stocky plate/stiffeners with $\sigma_{yE} >> \sigma_Y$ the equivalent bending stress is small).

The equivalent pressure due to the transverse stress becomes

$$p_{\sigma_y} = \frac{12W_s\sigma_Y}{\ell^2 s\sigma_{yE}}\sigma_y \tag{3.120}$$

This may be written

$$p_{\sigma_y} = \frac{13.3W_s\sigma_Y}{2\left(1+\sqrt{1+\frac{10.9I_s}{t^3 s}}\right)Et^2 s}\sigma_y \tag{3.121}$$

For simply supported stiffeners the constant 13.3 is replaced by 8.9

Column buckling

The characteristic buckling strength of stiffeners and girders is based on a Perry-Robertson formulation using ECCS/Eurocode 3 buckling curve B, refer section 2.5.1, i.e.

$$\frac{\sigma_{xcr}}{\sigma_Y} + \frac{\sigma_{xcr}}{1-\frac{\sigma_{xcr}}{\sigma_E}}\frac{w_{eq}A}{\sigma_Y W} = 1 \tag{3.122}$$

A parameter μ is defined such that

$$\mu = \frac{w_{eq}A}{W} = \left(0.34 + 0.08\frac{z_p}{i_e}\right)\left(\bar{\lambda} - 0.2\right) \quad \text{for check at plate side}$$

$$\mu = \frac{w_{eq}A}{W} = \left(0.34 + 0.08\frac{z_t}{i_e}\right)\left(\bar{\lambda} - 0.2\right) \quad \text{for check at stiffener side}$$

The factor $\mu' = 0.34\left(\bar{\lambda} - 0.2\right)$ is identical to that applied for curve B in Eurocode. The second term accounts for the fact that the tolerance level for column imperfections in Eurocode is $w_{eq} = 0.001\ell$ while NORSOK allows imperfection of $w_{eq} = 0.0015\ell$ (ℓ is member length).

- -

Recalling Eq (2.47), the α factor implies an equivalent imperfection given by

$$\frac{w_{io}}{l} = \frac{1}{\pi}\sqrt{\frac{\sigma_Y}{E}}\frac{i}{z_o}\alpha\left(1-\frac{\bar{\lambda}_o}{\bar{\lambda}}\right)$$

For α = 0.34 the Eurocode equivalent imperfection is $w_{io} = 0.0037 i_e/z_0 \cdot \ell$ for σ_Y = 250 MPa and $w_{io} = 0.0045 i_e/z_0 \cdot \ell$ for σ_Y = 355

The term i_e/z_0 depends on the cross-section, but may typically be in the range of 0.5 – 1.0 for the top flange and 1 - 2 for the plate flange. Hence, the equivalent imperfection is larger for plate-induced failure, which may be consistent with the assumption used in Class Note 30.1

The second term can be written as

$$\frac{w_{io}}{l} = \frac{0.08}{\pi}\sqrt{\frac{\sigma_Y}{E}}\left(1 - \frac{\bar{\lambda}_o}{\bar{\lambda}}\right)$$

which gives an additional imperfection of $w_{io} = 0.0009 \ell$ for σ_Y = 250 MPa and $w_{io} = 0.001 \ell$ for σ_Y = 355 MPa (3.123)

- ----------

The critical axial stress comes out to be,

$$\frac{\sigma_{cr}}{\sigma_Y} = \frac{1 + \mu + \bar{\lambda}^2 - \sqrt{\left(1 + \mu + \bar{\lambda}^2\right)^2 - 4\bar{\lambda}^2}}{2\bar{\lambda}^2} \qquad \textbf{(3.124)}$$

where the reduced slenderness is defined by,

$$\bar{\lambda} = \sqrt{\frac{\sigma_Y}{\sigma_E}} \quad , \quad \sigma_E = \frac{\pi^2 E\, i_e^2}{l_e^2} \qquad \textbf{(3.125)}$$

As discussed in Section 2.9.3, if the torsional buckling stress is less than the yield stress ($\lambda_T \geq 0.6$) the yield stress shall be replaced by the torsional buckling stress.
In calculating the Euler buckling force, the effective buckling length must be determined. As described in Section 3.4.6 the buckling length depends on the lateral pressure. If the pressure is small the stiffener may be assumed to be simply supported on the frames and the buckling length is equal to the frame spacing. If the pressure is large, the stiffener may not not be able to snap through, and for symmetry reasons it may be considered as clamped at the frames. The buckling length is then equal to half of the frame spacing. In Norsok and DnV RP C201, it is assumed that the buckling length is a continuous function of the pressure according to the following expression:

$$\ell_e = \ell\left(1 - 0.5\frac{p}{p_Y}\right) \qquad \textbf{(3.126)}$$

where p_Y is the pressure causing first yield in the stiffener at the support;

$$p_Y = \frac{12 W \sigma_Y}{\ell^2 s} \qquad \textbf{(3.127)}$$

Failure for combined axial compression lateral pressure
For stiffeners subjected to combined axial compression and bending two failure modes have to be checked:

i. Combined axial compression and bending on the compression side
ii. Combined axial compression and bending failure on the tension side

In the case of lateral pressure on the plate side, the failure mode i) is to be checked at points 1 and 4, refer **Figure 3.1**. Failure mode ii) is to be checked at points 2 and 3.

Combined axial compression and compressive bending is checked according to the formula:

$$\frac{N}{N_{cr}} + \frac{M \pm Nz^*}{M_{cr}\left(1 - \frac{N}{N_E}\right)} = 1 \qquad \textbf{(3.128)}$$

where $N_{cr} = \sigma_{cr} A$ is the critical axial force for pure axial loading

$$M = \frac{1}{12} q\ell^2 \quad \text{stiffner supports}$$

$$M = \frac{1}{24} q\ell^2 \quad \text{mid span}$$

when the pressure is uniform. The critical bending moment, $M_{cr,}$ is assumed equal to the first yield moment the plate flange. On the stiffener side, torsional buckling of the stiffener needs to be checked. If the critical stress is less than the yield stress, the torsional buckling stress replaces the yield stress.

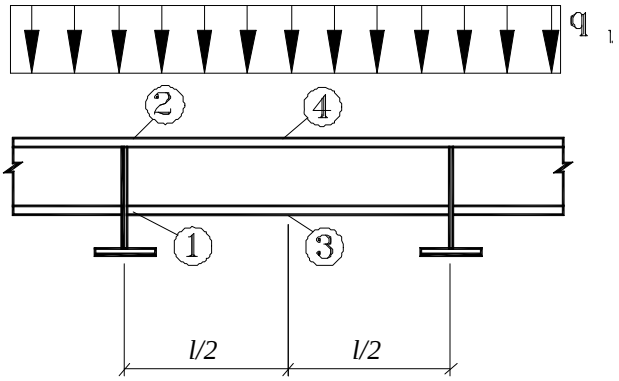

Figure 3.32 Check points for interaction equations (From NORSOK N-004/DnV RPC201)

z* represents the working point for the axial force relative to the neutral axis for the effective stiffener cross-section. This eccentricity causes a bending moment from the axial force which either adds to or counteracts the bending moment from the lateral load, refer **Figure 3.33**. The action at the support and at mid span will be opposite. Hence, for a certain value of z* the utilisation at mid span and the support will become equal. Failure is assumed to occur when the utilisation is equal to unity at both positions. The actual value of z* has to be determined by trial and error.

Figure 3.34 illustrates how the utilisation may vary for a given panel for vaying eccentricity. The optimum value (minimum utilisation) is obtained where the curves for utilisation at mid

span and the support intersects. If the eccentricity is neglected (z* = 0), one of the utilisations will be larger. Hence, it is always conservative to neglect the eccentricity

Ideally, when calculating the forces and moments in the total structure, of which the stiffened panel is a part, the working point for the stiffened panel should correspond to the assumed value of z*. In most cases the influence of variations in z* on global forces and moments will be negligible.

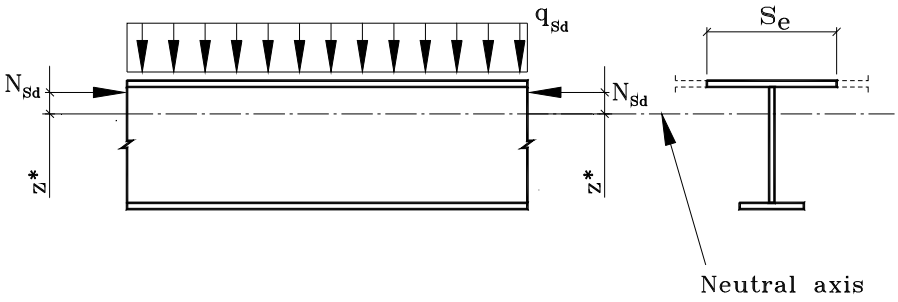

Figure 3.33 Definition of z^*. z^* is positive towards plate flange (From NORSOK N-004/DnV RPC201).

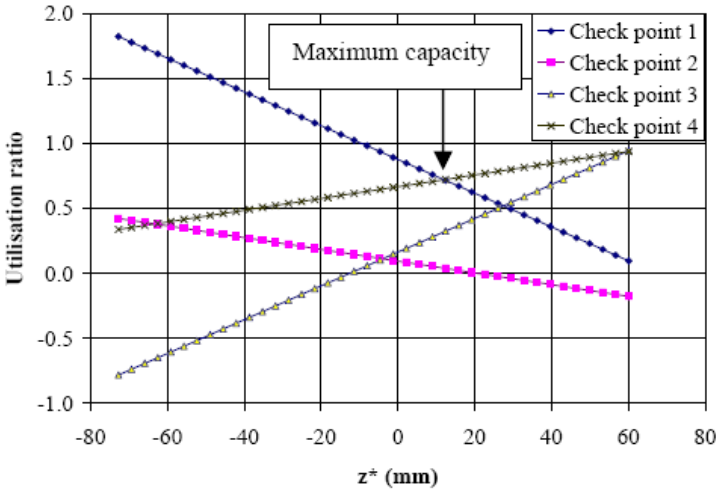

Figure 3.34 Utilization versus the eccentricity factor z^* (From DnV RPC201)

The second check is performed on the tension side of the stiffener in bending. Failure is based on linear interaction between utilization with respect to buckling and yielding, respectively.

If the stiffener is stocky, with a critical stress in the range of the yield stress, the first term is zero or negligible. Hence, pure tensile yielding is governing. For slender stiffeners, the first term becomes significant and reduces the allowable utilization in bending. The second term represents the utilization with respect to tensile yielding, and the compressive stress from the axial force must be subtracted.

$$\underbrace{\left(\frac{N}{N_{cr}}-\frac{N}{N_Y}\right)}_{\text{utilizatio wrt buckling}}+\underbrace{\left[\frac{M\pm Nz^*}{M_{cr}\left(1-\frac{N}{N_E}\right)}-\frac{N}{N_Y}\right]}_{\text{utilization wrt yielding}}=1 \qquad \textbf{(3.129)}$$

or

$$\frac{N}{N_{cr}}-2\frac{N}{N_Y}+\frac{M\pm Nz^*}{M_{cr}\left(1-\frac{N}{N_E}\right)}=1 \qquad \textbf{(3.130)}$$

where

$N_Y = \sigma_Y A_e$ is the yield force of the effective cross-section
$N_{cr} = \sigma_{cr} A_e$ is the critical stress for pure axial compression

3.4.7 Resistance of girders

The resistance of girders is in NORSOK N-004/DnV RPC201 calculated in the same manner as stiffeners. The effective flange of the girder ℓ_e, needs to be estimated. Expression similar expression those for plates are used. A crucial issue is whether the stiffeners are effective against transverse compression. If this is the case, the reduction due to stress in x-direction is based upon effective width of long plates according to Equation 3.29. If not the effective flange in y-direction is calculated neglecting the stiffeners.

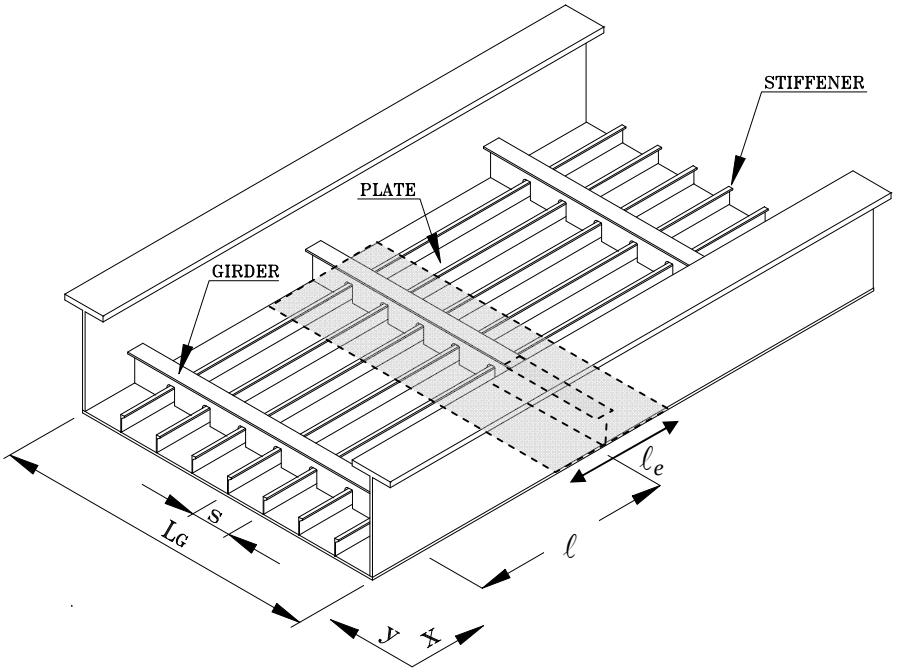

Figure 3.35 **Effective plate flange for girder** (Reproduced from NORSOK N-004/DnV RPC201).

3.4.8 Tripping of Stiffeners

The tripping problem is a complicated phenomenon to analyze analytically. Most of the methods do not account for this failure mode which also shows a violent unloading in the post-collapse region. Hence, tripping failure is normally avoided by designing the stiffeners with limited slenderness. For flat bar stiffeners, the thickness-height ratio should satisfy the following expression,

$$\frac{h_w}{t_w} \le C\sqrt{\frac{E}{\sigma_y}} \tag{3.131}$$

where $C = 0.35 \sim 0.37$.

3.5 Grillage Buckling

3.5.1 Elastic Analysis

As previously mentioned, grillage buckling is in most cases avoided by designing the structure with a sufficient margin against this failure mode. It is very complicated to analyze the real collapse behaviour of grillages including inelastic effects, large deflection, load-redistribution effects, and interaction between local and overall instability. Thus, most analytic work has been confined to the elastic range. In the following, the energy method is used to calculate the elastic buckling load of an orthogonally stiffened panel with pinned edges, (Figure 3.36). The displacement field is assumed to be,

$$w = C_{mn}\sin\frac{m\pi x}{a}\sin\frac{n\pi y}{b} \tag{3.132}$$

which satisfies the essential boundary conditions.

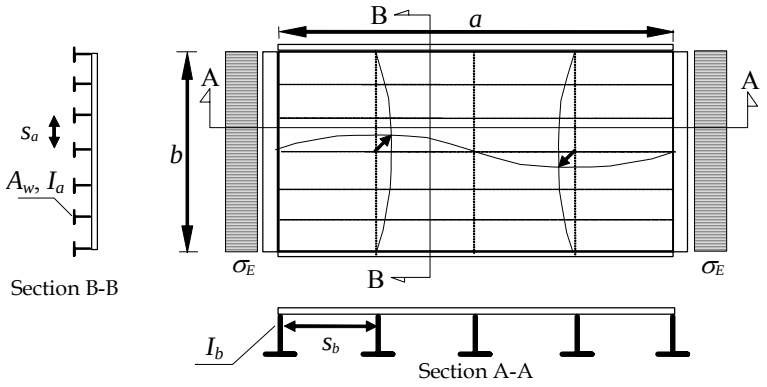

Figure 3.36 Buckling of an Orthogonally Stiffened Panel with Pinned Edges.

The elastic strain energy stored in the plates is given by,

$$U = U_p + \sum_{i=1}^{q} U_a^i + \sum_{i=1}^{q} U_b^i \tag{3.133}$$

The contribution from the plate is,

$$U_p = \frac{D}{2}\iint \left(\nabla^2 w\right)^2 dxdy \tag{3.134}$$

while the contribution from the longitudinal stiffeners and the transverse girders are respectively,

$$U_a^i = \frac{EI_a}{2}\int \left(\left.\frac{\partial w}{\partial x}\right|_{y_i} \right)^2 dx \tag{3.135}$$

$$U_b^i = \frac{EI_b}{2}\int \left(\left.\frac{\partial w}{\partial y}\right|_{x_i} \right)^2 dy \tag{3.136}$$

The potential energy of the external compressive load is still given by Equation (3.10). The critical load is found by setting the variation of the total potential energy equal to zero. The solution can be written as follows,

$$\sigma_E = \frac{\pi^2 D}{b^2\left(t + \delta_a t_a\right)}\left[\left(\frac{mb}{a} + \frac{a}{mb} \right)^2 + i_a \left(\frac{mb}{a} \right)^2 \delta_a + i_b \left(\frac{a}{mb} \right)^2 \delta_b \right] \tag{3.137}$$

where δ_a and δ_b have the following meanings:-

$$\delta_a \ \langle \delta_b \rangle = \begin{cases} 0 & when\ axial\ (transverse)\ stiffeners\ take\ part\ in\ deflection \\ 1 & when\ axial\ (transverse)\ stiffeners\ don't\ take\ part\ in\ deflection \end{cases}$$

when longitudinal stiffeners (transverse girders) are not deflected.

The following notations are used,

$t_a = \dfrac{A_w}{s_a}$: equivalent thickness of longitudinal stiffeners (plate flange not included)

$i_a = \dfrac{EI_a}{Ds_a}$: relative stiffness of longitudinal stiffeners (with effective plate flange)

$i_b = \dfrac{EI_b}{Ds_b}$: relative stiffness of transverse girders (with effective plate flange)

Example 3.1

What is the necessary moment of inertia of the transverse girders, I_b, to assure buckling of longitudinals between transverse girders?

Solution:

Except for very lightly stiffened panels, the first term in Equation (3.121) can be disregarded. Therefore, for overall buckling,

$$\sigma_{E,g} = \frac{\pi^2 D}{b^2(t+t_a)}\left[i_a\left(\frac{mb}{a}\right)^2 + i_b\left(\frac{a}{mb}\right)^2 \right]$$

The minimum buckling load is found by differentiating with respect to *m*, yielding

$$\sigma_{E,g} = \frac{\pi^2 D}{b^2(t+t_a)}\left[2\sqrt{i_a i_b}\right]$$

For inter-frame flexural buckling of stiffeners one obtains,

$$\sigma_{E,a} = \frac{\pi^2 D}{b^2(t+t_a)}\left[i_a\left(\frac{mb}{a}\right)^2 \right] \quad ; (m=4)$$

In the limit, $\sigma_{E,g} = \sigma_{E,a}$, gives

$$i_b = \frac{1}{4}\left(\frac{mb}{a}\right)^4 i_a$$

Assume that there are two longitudinal stiffeners and four transverse girders ($m = 5$). This yields the following requirement to the moment of inertia of the transverse girders,

$$I_b = \frac{3^4}{4}\left(\frac{s_a}{s_b}\right)^3 I_a$$
$$= 20.25\left(\frac{s_a}{s_b}\right)^3 I_a$$

3.6 References

1. Guedes Soares, C. and Søreide, T.H.:
"Behaviour of Stiffened Plates under Predominantly Compressive Loads".
International Shipbuilding Progress, Vol. 30, Jan., 1983.

2. "*Buckling Strength Analysis*", Classification Note No. 30.1,
Det Norske Veritas, 1982.

3. Faulkner, D.:
"*A Review of Effective Plating for Use in the Analysis of Stiffened Plating in Bending and Compression*". Journal of Ship Research, Vol. 19, 1975.

4. Faulkner, D.:
"*Design Against Collapse for Marine Structures*".
International Symposium on Advances in Marine Technology, Trondheim, 1979.

5. Frieze, P.A., Dowling, P.J. and Hobbs, R.H.:
"*Ultimate Load Behaviour of Plates in Compression*".

Steel Plated Structures, Crosby Lockwood Staples, London 1977.

6. Carlsen, C.A. and Czujko, J.:
"*The Specification of Tolerances for Post-Welding Distortion of Stiffened Plates in Compression*".
The Structural Engineer, Vol. 56A, No.5, May 1978.

7. Søreide, T.H. and Czujko, J.:
"*Load Carrying Capacities of Plates Under Combined Lateral Load and Axial/Biaxial Compression*".
2nd International Symposium on Practical Design in Shipbuilding, Tokyo/Seoul, 1983.

8. Valsgård, S.:
"*Numerical Design Prediction of the Capacity of Plates in Biaxial In-Plane Compression*".
Computer and Structures, Vol. 12, No. 5, 1980.

9. Harding, J.E. and Dowling, P.J.:
"*The Basis of the Proposed New Design Rules for the Strength to Complex Edge Loading*".
Stability Problems in Engineering Structures and Components, Applied Science Pub., London, 1979.

10. Rules for the Design, Construction and Inspection of Offshore Structures, Appendix C, Det Norske Veritas, 1977.0

INDEX